Chemical Engineering Science, Volume 248, Part B, February 2022, Article number 117218
DOI:10.1016/j.ces.2021.117218

Non-Invasive Measurement of Oil-Water Two-Phase Flow in Vertical Pipe Using Ultrasonic Doppler Sensor and Gamma Ray Densitometer

Baba Musa Abbagoni*[, 1, 2] **Hoi Yeung[1]** **and Lao Liyun[1]**

[1]Energy and Power, Cranfield University, MK43 0AL, United Kingdom

[2]Department of Electrical and Electronic Engineering, University of Maiduguri, PMB 1070, Bama Road, Maiduguri, Nigeria

***Corresponding author. E-mail address**: bamusa08@gmail.com

Abstract

Oil–water two-phase flow experiments were conducted in a vertical pipe to study the liquid-liquid flow measurement using a non-invasive ultrasound Doppler flow sensor and a gamma densitometer. Tap water and a dyed mineral oil are used as test the fluids. A novel Doppler effect strategy is used to estimate the mixture flow velocity in a vertical pipe based on flow velocity measured by the ultrasound sensor and the shear flow velocity profile model. Drift-flux flow model was used in conjunction phase fractions to predict the superficial velocities of oil and water. The results indicate that the proposed method estimated oil-continuous flow and water-continuous flow have average relative errors of 5.2% % and 4.5%; and superficial phase flow velocities of oil and of water have average relative errors of 4.5% and 5.9% respectively. These results demonstrate the potential for using ultrasonic Doppler sensor combined with gamma densitometer for oil-water measurement.

Keywords:

liquid-liquid flow; drift-flux model; velocity profile; water fraction, phase superficial velocity

Published by Elsevier. This is the Author Accepted Manuscript issued with: Creative Commons Attribution Non-Commercial No Derivatives License (CC:BY:NC:ND 4.0).
The final published version (version of record) is available online at DOI:10.1016/j.ces.2021.117218. Please refer to any applicable publisher terms of use.

1 Introduction

Oil-water two-phase flow is frequently encountered in the petroleum industry, for example, in transportation pipelines between production wells and offshore platform separators (Eskin et al., 2017). Accurate measurement of the oil-water two-phase flow is very important and challenging for a range of applications, particularly for reservoir assessment and management (Du et al., 2012), liquid production prediction and control(Shi et al., 2017), produced water estimation and management (Zhai et al., 2013). Importantly, as a oil field matures, the amount of water that would be produced together with the oil in the well increases significantly (Hasan and Kabir, 1998; Lucas and Jin, 2001). The high water-cut oil-water flow causes a serious challenge to most multiphase flow measurement instruments such as the device has to deal with are the influences of small density difference between oil and water, flow regime and kinematic viscosity. The differences in flow regimes is created by the Kinematic viscosity (Dong et al., 2015).

Several attempts at measuring oil-water two-phase flow in both horizontal and vertical pipe using either a single or multiple instruments were successful (Shamsul et al., 2015). Single sensing device is often use in measuring a parameter of flow such as velocity, phase volume fraction, pressure gradient, flow pattern identification and characterisation(Shamsul et al., 2015). For example, sensors frequently used in measuring oil-water flow include pressure transducers (Da et al., 2007; Flores et al., 1998; Shamsul et al., 2015), ultrasonic sensors(Dong et al., 2015; Kouame et al., 2003; Morriss and Hill, 1991; Tan et al., 2016), gamma densitometer(Descamps et al., 2006; Kumara et al., 2010a; Tesi, 2011), conductance probes(Chen et al., 2015; Du et al.,

2012; Jana et al., 2006; Oddie, 1992; Shamsul et al., 2015) capacitance probes(Ismail et al., 2005) and electromagnetic flowmeters(Faraj et al., 2015; Jin et al., 2020).

As a matter of fact, a comprehensive measurement of two-phase flow requires use of at least two different devices or two independent outputs of one device. Experimental studies on measurement of oil–water flow using two-sensor methods are plenty. For example, Conductance Ring Coupled Cone (CRCC) meter (Tan et al., 2015), electromagnetic flowmeter(EMFM) and electrical resistance tomography (ERT)(Faraj et al., 2015), EMFM combined with a plug-in conductance sensor array (PICSA)(Jin et al., 2020), electrical capacitance tomography and venturi tube (Liu et al., 2017), ultrasonic transducers and electrical sensors(Tan et al., 2016), ultrasonic transducer and venturi tube(Huang et al., 2013), and gamma-ray densitometer and electrical conductivity probes (Descamps et al., 2006) have been reported in the literature.

In addition, data fusion of several sensor signals and physical model of the multiphase flow for real time measurement of oil, gas and water flow rates in a three phase flow was successfully implemented by Meribout et al., (2010). Similarly, Figueiredo et al., (2016) reported an oil-continuous multiphase flow measurement method by using acoustic attenuation data for generating data for neural networks model for flow pattern recognition as well as gas volume fraction (GVF) estimation. But the downside of this type of multi-sensor multiphase flowmeters that it first involves features extraction and data training, and it uses invasive sensors which may incur pressure loss and higher installation or retrofit costs.

Conductance sensor, even though it is an intrusive device, has been widely used for measuring the phase fraction or the flow velocity of oil-water two-phase flow (Chen et al., 2015). It records the time-varying electrical conductive characteristics of the oil–

72 water flow, However, conductance sensors are significantly affected by phase inversion
73 when flow changes from water-continuous flow to oil-continuous flow, the detection
74 has to change from conductance to capacitance (Figueiredo et al., 2016). In a similar
75 way, electrical capacitive sensors, though non-invasive, are susceptible to coating by
76 paraffin wax and affected by the phase inversion as well, when the flow changes to
77 become conductive as in water continuous-flow (Chaudhuri et al., 2014; Dong et al.,
78 2015). Moreover, turbine flowmeter and Venturi tube are intrusive instruments and so
79 they can cause flow constriction or contribute to pressure losses. A Non-invasive two-
80 phase flowmeter eliminates causes of pressure drop and corrosion of sensor, and
81 importantly, it will help to reduce installation cost and maintenance cost (Kumara et al.,
82 2010a). Ultrasonic Doppler technique is good choice for two-phase flow measurement
83 as it operates without flow disturbance and not restricted by pipeline material(Yin et al.,
84 2019).

85 Ultrasonic techniques have been widely used for both phase velocity and phase fraction
86 measurements (Thorn et al., 2013). The ultrasonic Doppler techniques have been
87 explored for velocity measurement are the pulsed-wave ultrasonic Doppler(PWUD) and
88 continuous-wave ultrasonic Doppler(CWUD) (Tan et al., 2021). PWUD utilises a single
89 transducer to intercept the moving stream by sending short ultrasonic burst and
90 receiving echoes from tracer particle along a sound beam. A typical example of such a
91 sensor is described by (Baker and Yates, 1973; Murai et al., 2010; Yin et al., 2019). The
92 CWUD uses two separate transmitting and receiving transducers to measure the
93 average flow velocity(Abbagoni and Yeung, 2016; Brody et al., 1974; Dong et al.,
94 2016, 2015; Tan et al., 2021). Although measurements obtained by PWDU devices are
95 perfectly adequate for flow measurement, maximum flow velocity can be measured

with the PWDU is limited by its sampling frequency (Tan et al., 2021). The CWDU technique can accurately measure flow velocity of oil-water two-phase flow and theoretically, there is no maximum limit to the subsonic flow velocity it can measure.

In fact, the non-invasive continuous wave Doppler ultrasound (CWDU) system was first invented for medical application in 1957 by Satomura, and in particular, the CWDU sensor is being developed for various flow measurement ever since. Kouame et al., (2003) presented an application of CWDU sensor for two phase flow velocity measurement and proposed the use of high resolution frequency techniques to overcome the problem of coloured noise. Shi et al., (2017) applied CWDU sensor technique to study oil-water flow in horizontal pipe and developed a model which takes into the influence of holdup distribution in determining the overall superficial flow velocity. Dong et al., (2015) developed a method of measuring oil-water two-phase flow using CWDU transducers and a generalised two-phase oil-water flow model. However, there was no consideration of hybrid sound velocity to compensate for the changes in sound velocity in the oil-water mixture flow. This may reduce the accuracy of the method. Similarly, Tan et al., (2016) developed a two-phase oil-water flow measurement model for a combined two sensor system of CWDU transducers and electrical sensors and studied oil–water two-phase flow through horizontal pipe experimentally for estimating the mixture flow velocity.

However, oil–water vertical flow measurement using ultrasonic Doppler methods are rather scanty. In order to measure mixture flow velocity of liquid-liquid flow such as the oil-water using the ultrasonic Doppler sensor, a theoretical model would be needed to supplement the CWDU sensor measurements. As examples, such mathematical models have been developed for horizontal oil-water flow in the literatures (Dong et al., 2016,

120 2015; Liu et al., 2021; Tan et al., 2016). Table 1 presents recent experimental works for
121 oil–water flow measurements. a more elaborate survey over ultrasonic Doppler
122 methods for multiphase flow measurement can be found in Tan et al., (2021).

123 **Table 1** Recent experimental works for oil–water flow measurement

	Tan et al., (2016)	Mazza and Suguimoto, (2019)	Liu et al., (2021)	Jin et al., (2020)
Oil density, kg/m^3	841	793	790	Not stated
Oil viscosity, (Pa.s)	0.0147	0.0011	0.029	Not stated
Pipe diameter (mm)	50	26	50	20
Pipe orientation	Horizontal	Vertical	Horizontal	Horizontal
Superficial velocities, m/s	Yes	No	No	Yes
Water fraction/holdup measurement	Yes	Yes	No	Yes
Flow pattern identification	No	Yes	Yes	Yes
Sensing device(s)	Ultrasonic transducers & conductance/capacitance sensor	Pressure transducer and impedance probe	Ultrasonic sensor and conductance sensor	Electromagnetic flowmeter and conductance sensor

124

125 From the table it is clear that only Mazza and Suguimoto, (2019)Mazza and Suguimoto,
126 (2019) performed experimental oil-water vertical flow measurement but they use
127 pressure transducers and impedance probes. Jin et al., (2020) Jin et al., (2020)studied
128 vertical low-velocity oil-water two-phase horizontal flow using electromagnetic
129 flowmeter and conductance sensor and stated that non-uniform conductivity distribution
130 leads to error for the output of the EMF. Liu et al., (2021) investigated experimentally
131 the flow pattern identification of oil-water horizontal flow using ultrasonic transducer

and conductance sensor but do not provide holdups and superficial flow velocities. The above-mentioned studies have shown not just the strengths of the ultrasonic Doppler technique but also a necessity for establishing a theoretical model for measurement of oil-water two-phase using the CWDU sensor. However, most of the ultrasonic Doppler methods are limited to horizontal flow and the phase fraction data were obtained with conductance sensor- an intrusive device!

Gamma densitometer is also a non-invasive sensing device that is often used in measuring phase volume fraction and mixture flow density (Descamps et al., 2006; Kumara et al., 2010a). Descamps et al., (2006) measured the density of oil–water flow through a vertical tube and in situ liquid (oil and water) hold up, using a Berthold LB 444 gamma ray densitometer. Kumara et al., (2010a) experimentally investigated oil-water flow in a 15 m long, 56 mm diameter horizontal and slightly inclined pipes and measured the time averaged cross-sectional distributions of oil and water with by traversing a single-beam gamma densitometer along the vertical pipe diameter.

The above survey revealed that the ultrasound Doppler sensor and the gamma-ray densitometer are right choice for a non-invasive multiphase flow measurement system. Experimental results reported in the literatures on the studies of liquid-liquid flow measurement also showed that there is little research available on the use of clamp-on (non-invasive) ultrasonic Doppler method to measure oil-water two-phase flow, especially in the vertical pipe. A Non-invasive technique can be used as a temporary, semi-permanent or permanent method of multiphase flow measurement(Sanderson and Yeung, 2002).

Measurement of the phase flowrates is an important part of managing oil production and besides, it is a necessary prerequisite for water disposal and/or water

156 reinjection(Faraj et al., 2015). However, the majority of the studies in oil-water flows
157 are confined to horizontal pipes and the flow patterns in the vertical oil-water two-phase
158 flow are entirely different from that of the horizontal flow systems. The motivation
159 behind the present study is to perform an experimental study on oil-water two-phase in
160 vertical upward flow pipe using non-invasive Doppler ultrasonic methods for
161 measurement of the phase flow rates.
162 In the present study, firstly it is focused on measuring the superficial the mixture flow
163 velocity with the CWDU sensor conjunction with a theoretical flow velocity profile
164 model, and the water volume fraction using the gamma-ray densitometer this paper, a
165 non-invasive method to estimate the mixture flow velocity and The mixture flow
166 velocity encompasses both laminar and turbulent velocity profiles to represent the two
167 main flow regimes of oil-continuous flow and water-continuous flow respectively.
168 Secondly, the drift-flux model will be modified to estimate the superficial flow
169 velocities of oil and of water from the data obtained by measuring the mixture flow
170 velocity and calculating the water volume fraction. The estimated results will be
171 compared with single phase flow meters at the inlets of the test rig. The difference
172 between the test flowmeters and the reference flowmeters will be discussed along the
173 effects of the phase volume fraction on the measurement results.

174

175 # 2 Measurement Methodology

176 ## 2.1 Ultrasound Doppler principle

177 A CWDU sensor uses the Doppler effect principle for the of flow measurement, in
178 which both the ultrasound signal transmitter and receiver transducers are stationary but
179 former sends ultrasound waves to and latter receive scattered waves from the moving

scatterers (droplets) in the flow. The average the droplets velocity in the measuring volume of the CWDU flowmeter sensor $\bar{v}$ is determined using the Doppler effect principle as (Brody et al., 1974; Shi et al., 2017). Details on the interaction of the ultrasound wave with the oil-water flow can be found in (Dong et al., 2015a; Liu et al., 2021; Tan et al., 2021; Zhai et al., 2013).

The received ultrasound from a point droplet is a sinusoidal signal shifted in frequency from the transmitted ultrasonic carrier by an amount f_d. The f_d is related to the classical Doppler shift formula(Brody et al., 1974):

$$\bar{v} = \frac{c\overline{f_d}}{2\, f_t cos\, \theta} \tag{2-1}$$

where: c is the speed of sound, $f_t$is the transmitted ultrasonic carrier frequency, θ is the transducer orientation angle and $\overline{f_d}$ is the average frequency shift reflected by multiple droplets in the flow.

Although, there are some very small gas bubbles in the oil-water flow which could also scatter the ultrasound which may complicate the measurement. The present method assumes that the two-phase flow is well-mixed and the air particles in the flow are infinitesimally small compared to the wavelength of sound, and the effects of scattering by gas-bubble is neglected (Chaudhuri et al., 2014; Garcia-Lopez and Sinha, 2008).

In oil-water two-phase flow, nevertheless, the Eqn. (2-1) could still be susceptible to errors due to the different sound speed in oil and in water (Dong et al., 2015). Therefore, the sound speed in the oil/water mixture is a hybrid sound speed c_{ow} which can be obtained from the Urick(1947) model, as follows (Garcia-Lopez and Sinha, 2008):

$$c_{ow} = \frac{1}{\sqrt{\rho_m^2 k_m}} \tag{2-2}$$

The variables ρ_m and k_m denote the mixture density $\rho_m = \rho_w\alpha_w + (1-\alpha_W)\rho_o$ and the mixture compressibility $k_m = k_w\alpha_w + (1-\alpha_W)k_o$.

where α_w is the phase volume fraction of water ,k_w is the compressibility of water and k_o is the compressibility of oil respectively, and ρ_w and ρ_o denote density of the oil and the water, respectively.

Equation (2-2) is an appropriate result for estimation of the sound speed in the mixture flow. Rewriting Eqn. (2-1):

$$\bar{v} = \frac{c_{ow}\overline{f_d}}{2\, f_t cos\, \theta} \tag{2-3}$$

Equation (2-3) shows the expression of the flow velocity under the assumption that the transducers are uniformly transmitting and receiving ultrasonic signal into and from the flow and homogeneous distribution of the droplets in the flow. The flow velocity can computed and subsequently, the average flow rate can be estimated; knowing the cross-section area of the pipe (Brody et al., 1974).

The droplets are travelling at different velocities and the received Doppler signal contains a distribution of frequencies which can produce a spectrum. So, the Doppler signal can be analysed through to the spectral estimation. The average Doppler frequency shift $\overline{f_d}$ was calculated from a power spectrum using an intensity-weighted-mean (IWM) equation(2-4) (Morriss and Hill, 1991).

$$\overline{f_d} = \frac{\int_0^{f_{max}} P(f) f df}{\int_0^{f_{max}} P(f) df} \tag{2-4}$$

where: f_{max} is the maximum Doppler frequency, $P(f)$ is the Doppler power spectrum, $\overline{f_d}$ is the average Doppler shift, f_t is the transmitted frequency and f is the Doppler frequency shift

220 The CWDU sensor may be used to measure the flow velocity in the whole pipe cross
221 section. However, the sensing volume of the CWDU sensor is fixed region(often it does
222 not cover the whole pipe cross-section) in the in pipe through which moving droplets
223 will cause a detectable Doppler-shifted signal(Baker and Yates, 1973) A rule of thumb
224 to follow is not to choose ultrasound sensor with measuring volume larger than is
225 necessary. This is to avoid ultrasound signal reflection through the pipe walls which is a
226 major concern. Other constraints include:(1) if the transducer were designed to have
227 bigger dimensions so as to produce larger measuring volume, then the origin of echoes
228 may come from the pipe walls as well. (2) if the if the sample volume is too small only
229 a uniform flow profile (i.e., plug flow) can be accurately measured(Rothfuss et al.,
230 2016). The measurement volume of the present method and pipe diameter is described
231 in the section3.3. The capability of the CWDU sensor for flow velocity measurement
232 can be improved as described by the recent development of CWDU sensor through a
233 theoretical correlation by Dong et al., (2015a) and Tan et al., (2016).

234 The mean velocity V_m can be estimated by integrating the flow velocity in the
235 measuring volume. Based on these assumptions: (i) the ultrasonic intensity in the
236 measuring volume is homogeneous, and (ii) the distribution of droplets is homogeneous
237 in the measuring volume (Kikura et al., 2004). For oil-water flow measurement using
238 the Doppler measurement effective flow models is necessary to integrate the Doppler
239 shift frequency to handle the complex flow distribution(Tan et al., 2021). For example,
240 .Dong et al., (2015) carried out experiments with oil-water two-phase flow in a
241 horizontal pipe and used a mathematical Doppler model for combining the flow velocity
242 profile and the measured flow velocity in the measuring volume for measuring the
243 mixture flow. suggested a boundary layer model for describing the velocity profile of

dispersed and stratified oil-water flow for predicting superficial flow velocity and the flow velocity profile, measured flow velocity by ultrasonic sensor and phase fraction data were all combined to the predict the superficial flow velocity of each phase. Measurement of superficial flow velocities of oil and water in oil-water vertical pipe was not included in their work. In another development, Dong et al., (2016) described a method of incorporating the mathematical Doppler model (described in (Dong et al., 2015)) into the drift-flux model, based on the assumption that there is slippage between two phases, and the they found that the overall measurement error was reduced by 2.27%. However, these studies were conducted in horizontal pipes, and besides, the phase fraction was measured with electrical conductance sensor. Therefore, we extend that the method of mathematical Doppler model with the ultrasonic Doppler sensor for estimating the mixture oil-water flow to include estimation of the superficial flow velocity of oil and water from the measured mixture flow velocity.

2.2 Gamma ray densitometry

The gamma ray densitometer measurement theory is based upon electromagnetic radiation passing into the material is received by a detector. The emission and reception of the gamma electromagnetic radiation is governed by the Beer–Lambert's law (Kumara et al., 2010a):

$$I = I_0\, exp(-\varphi z). \tag{2-5}$$

where I_0 is the initial intensity, $(\text{photon}/\text{m}^2 - \text{sec})$, φ is the linear absorption coefficient; z is the distance travelled through the absorbing medium and I is the intensity of the gamma beam received at the detector.

Falcone et al., (2009) described a model of attenuation of gamma radiation across the pipe filled up with a multiphase flow for deriving the expression for the phase volume

fractions. The multiphase flow in a pipe is modelled as a square channel filled with oil and water with oil-water two-phase as shown in Figure 2-1(Kumara et al., 2010a; Stahl and von Rohr, 2004). a similar methodology for the for derivation of the expression for the phase volume fractions is adopted here.

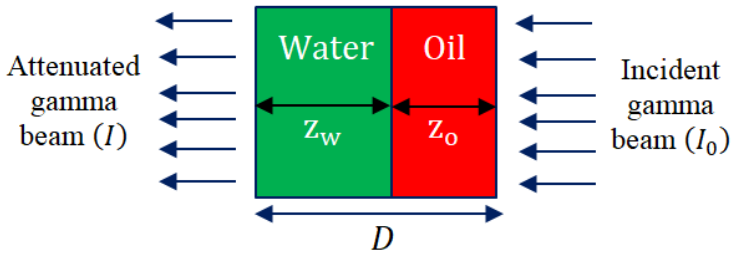


Figure 2-1 Attenuation of gamma radiation in a square channel filled with oil and water

Assume that there are two phases in the channel (e.g. oil and water) with path lengths for the gamma beam traversing the respective phases of z_o and z_w. The intensity I of the gamma beam received at the received at the detector is given by:

$$I = I_0 \exp(-\varphi_p z_p) \exp(-\varphi_a z_a) \exp(-\varphi_w z_w) \exp(-\varphi_o z_o) \quad (2\text{-}6)$$

where φ_p = linear absorption coefficient in the tube wall material; z_p = path length through wall; φ_a = linear absorption coefficient for air; z_a path length through air; φ_o, and φ_w = linear absorption coefficient for oil and water phases respectively.

For the two-phase mixture, the common method of calibrating the gamma densitometer is to measure the intensities (I_o and I_w) when the channel is full of each respective phase. Thus,

$$I_o = I_0 \exp(-\varphi_p z_p) \exp(-\varphi_a z_a) \exp(-\varphi_o D) \quad (2\text{-}7)$$

$$I_w = I_0 \exp(-\varphi_p z_p) \exp(-\varphi_a z_a) \exp(-\varphi_w D) \quad (2\text{-}8)$$

Normally, the absorption in air is negligible.

Referring to Eqns. (2-6), (2-7) and (2-8), these give the test volume fractions for perpendicular phase distribution along the path length of the gamma beam as:

$$\alpha_o = \frac{z_o}{D} = \frac{ln(I/I_w)}{ln(I_o/I_w)} \tag{2-9}$$

$$\alpha_w = \frac{z_w}{D} = \frac{ln(I/I_o)}{ln(I_w/I_o)} \tag{2-10}$$

2.1 Two-phase flow regime models

Oil–water two-phase flow can be grouped into 1) the water continuous flow and 2) the oil continuous flow based on the flow rates and phase volume fraction. In oil-water two-phase flow, the Reynolds numbers of water-continuous flow is high and presumably turbulent flow but most oil continuous flow has a low Reynolds number and it is assumed that the flow will be laminar(Dong et al., 2015).

2.1.1 Laminar flow velocity profile

For a laminar vertical flow, the mean velocity(V_m,) and its maximum velocity(V_{max}) and the parabolic solution for laminar flow velocity profile$\left(u(r)\right)$ in circular pipe can be expressed as:

$$u(r) = -\frac{R^2}{4\mu}\left(\frac{dP}{dx} + \rho_m g\, sin\, \Phi\right)\left(1 - \frac{r^2}{R^2}\right) \tag{2-11}$$

$$V_m = \frac{2}{R^2}\int_0^R u(r)\, r dr = -\frac{R^2}{8\mu}\left(\frac{dP}{dx} + \rho_m g\, sin\, \Phi\right) \tag{2-12}$$

$$V_{max} = -\frac{R^2}{4\mu}\left(\frac{dP}{dx} + \rho_m g\, sin\, \Phi\right) \tag{2-13}$$

where y is the distance from the pipe centreline, R is the pipe radius, μ is the flow viscosity, $\frac{dP}{dx}$ is the axial pressure gradient, ρ_m is the mixture density, g is the

299 acceleratioin due to gravity and Φ is the angle of inclination of the flow pipe from the
300 horizontal.
301 For oil-continuous flow measurement,(V_{o-m}), is the mean velocity, and(V_{omax}) is its
302 maximum velocity. The mean velocity in the measuring volume $\bar{v}$ can again be
303 expressed as in Eqn.(2-12)

$$\bar{v} = \frac{\int_0^{\mathrm{r}} \left(1 - \frac{y^2}{R^2}\right) 2\pi y \, dy.}{\pi \mathrm{r}^2} . V_{omax} = V_{omax}\left(1 - \frac{\sigma^2}{2R^2}\right) \quad (2\text{-}14)$$

304 where σ is the radius of the measuring volume
305 Equation (2-3) is for the calculation of the local velocity which is the average velocity
306 of the scatterers in the measuring volume. The CWDU sensors can only measures the
307 local velocity directly but not the true mean flow velocity. However, the mean velocity
308 can be determined by establishing a theoretical relationship between the local flow
309 velocity and the flow velocity profile. The measuring volume of a CWDU sensor is a
310 fixed region in the flow pipe where the transmitting and receiving ultrasound beams
311 intersect as a result of a presence of detectable moving scatterers (Baker and Yates,
312 1973; Rothfuss et al., 2016). Figure 2-2shows the relationship between the measuring
313 volume and flow. The measuring volume shape and size is determined by the
314 dimensions of the piezoelectric chip and the geometry of the intersections of transmit
315 and receive ultrasound beams as suggested by Dong et al., (2015a).
316

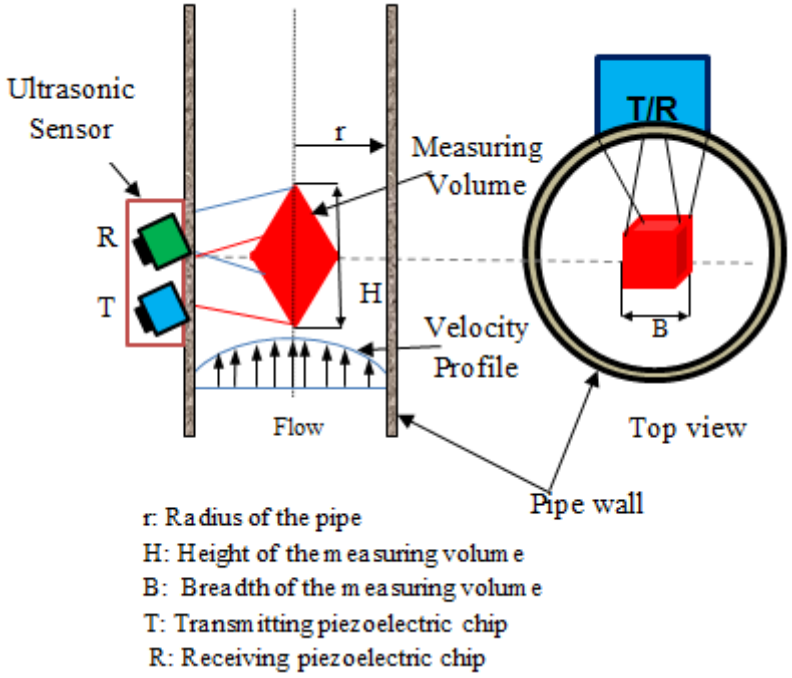


Figure 2-2 Relationship between the flow and the measuring volume

The mean velocity of the flow laminar oil-continuous flow in across the flow pipe is expressed as

$$V_{o-m} = \frac{\int_0^R \left(1 - \frac{y^2}{R^2}\right) 2\pi y \, dy.}{\pi R^2} . V_{omax} = \frac{1}{2} V_{omax} \tag{2-15}$$

Eliminating the maximum velocity, V_{omax} between these two equations (2-14) and (2-15)gives an equation of the mean velocity of oil-continuous laminar flow V_{o-m}

$$V_{o-m} = \frac{R^2}{(2R^2 - \sigma^2)} . \bar{v} \tag{2-16}$$

2.1.2 Turbulent flow velocity profile

In addition to the laminar flow profile described above, the importance of the role played by turbulence in oil-water two-phase flow cannot be over emphasized. As an example, Hu et al., (2007) studied oil–water vertical dispersed flow in 38mm ID pipe to investigate the crucial role of the turbulence in the distribution, and mixing of the phases and its contribution in droplet/bubble formation and breakage. They found out

329 that the phase fraction and the velocity of the dispersed both affect the characteristics in
330 oil-water flow. Moreover, Paolinelli, (2020) proposed a mechanistic model for stability
331 of dispersed oil-water flow in horizontal and inclined pipes and the h the model was
332 tested to be able to predict the break-up of dispersed phase droplets, and accumulation
333 of droplets.

334 In this work, we present an investigation on turbulent flow regime as well. Velocity
335 distribution in a pipe of a turbulent-flow can be resolved by either using the power law
336 or from the logarithmic law. In the present study, the properties of the water-continuous
337 turbulent flow velocity profile is by application of the logarithmic-law because it is very
338 often in agreement with experimental data (Chemlou et al., 2009; Eskin et al., 2017;
339 Kumara et al., 2010c). The logarithmic-law for the velocity profile can be expressed as

$$u^+ = 2.5\ln y^+ + 5.5, \quad y^+ > 11.6 \tag{2-17}$$

340 In the analysis of turbulent velocity profiles using the logarithmic law of the wall, it is
341 easier to work with non-dimensionalised variables: $y^+$is a non-dimensionalised distance
342 defined as $y^+ = \frac{u_\tau y \rho_m}{\mu_m}$ and u^+ is a non-dimensionalised velocity and it is defined
343 as: $u^+ = u/u_\tau$, where u_τ is the shear velocity and it is defined in section 2.1.2.1. For a
344 circular pipe, $y = R - r$, where R is the pipe radius and r denotes the radial position
345 where the velocity is calculated, and y is the radial distance from the pipe wall.

346 Substituting the non-dimensionalised variables into Eq. (2-17), the Logarithmic-law
347 layer velocity profile of turbulent oil-water two-phase flow in a pipe can be expressed
348 as:

$$u_{ow} = 2.5u_\tau ln\left[\frac{(R-r)u_\tau \rho_m}{\mu_m}\right] + 5.5u_\tau \tag{2-18}$$

349 where u_τ is the shear velocity

2.1.2.1 Shear velocity model

The shear velocity u_τ can be expressed in terms of the wall shear stress and the mixture density.

$$u_\tau = \sqrt{\tau_w / \rho_m} = \sqrt{\frac{D}{4\rho_m} \cdot \frac{dP}{dx}} \tag{2-19}$$

where τ_w is the shear stress at the pipe wall, ρ_m is the density of oil-water mixture D is the pipe's internal diameter and $\frac{dP}{dx}$ is pressure gradient

For fully developed flow, the total pressure gradient is the sum of the frictional pressure gradient, and the gravitational pressure gradient(Brauner, 2002; Rodriguez and Oliemans, 2006):

$$\frac{dP}{dx} = 2f_m \frac{\rho_m V_m^2}{D} - \rho_m g \sin \Phi \tag{2-20}$$

where V_m is the mixture flow velocity, f_m the Fanning's friction factor of the two-phase mixture and g is acceleration due to gravity.

The friction factorf_m can be estimated from a correlation given the fluid properties such as Reynolds number, mixture flow velocity, viscosity and density. For turbulent flow of Newtonian fluids, the friction factor can be obtained from the Moody diagram, or calculated from one of the experimental correlations such as the Colebrook equation and Blasius correlation suggested in the literature (Brauner, 2002;Descamps et al., 2006).

The Moody diagram is accepted and used charts in engineering but the pipes roughness may increase with use as a result of corrosion, scale build-up, and precipitation. Consequently, the friction factor may augment by a factor of 5 to 10(Çengel, 2007). Similarly, Colebrook combined the data for transition and turbulent flow in both smooth and rough pipes into the following implicit relation known as the Colebrook equation:

$$\frac{1}{\sqrt{f}} = -2.0log\left(\frac{\varepsilon/D}{3.7} + \frac{2.51}{Re\sqrt{f}}\right) \quad (2\text{-}21)$$

The Colebrook equation is equivalent to the Moody chart(Çengel, 2007). In addition, the Blasius correlation in smooth tubes is given as:

$$f_m = \frac{b}{Re^n}, \qquad 300 \leq Re \leq 100,000 \quad (2\text{-}22)$$

Coefficient b and exponent n are to be obtained experimentally so as to fit experimental pressure drop data. The *Re is* Reynolds number *Re* for two-phase flow is to be defined in section 3.6

In the literature, there are several correlations for the effective viscosity of liquid–liquid two-phase flow but those different expressions seem to have little impact on the homogenous model predictions because there are other factors involved (Grassi et al., 2008). Therefore, the effective viscosity μ_m for the oil-water flow was calculated using as the expression in the Eqn. (2-23) (Dong et al., 2015; Kumara et al., 2009; Tan et al., 2016).

$$\mu_m = \alpha_w\mu_w + \alpha_o\mu_o \quad (2\text{-}23)$$

where μ_w and μ_o are the dynamic viscosities of water and oil respectively.

The mixture density, ρ_m, of the oil-water flow can be determined from the gamma-ray densitometer. From phase fraction can then be determine by

$$\rho_m = \rho_w\alpha_w + (1-\alpha_W)\rho_o \quad (2\text{-}24)$$

Substituting frictional pressure gradient and mixture density into the Eq. (2-19)produces Eqn.(2-25), hence the Shear velocity for the mixture vertical flow is

$$u_\tau = \sqrt{\left(\frac{D}{4\rho_m}\right).\left[2\left(\frac{b}{Re^n}\right)\frac{\rho_m V_m^2}{D} - \rho_m g\right]} \quad (2\text{-}25)$$

386 **2.1.2.2 Determining the mixture flow velocity**

387 The relationship between the average velocity of the flow droplets $\bar{v}$ and the shear
388 velocity u_τ is obtained by integrating the velocity profile over the area of the pipe.
389 Therefore,

$$\bar{v} = \frac{\int_0^R u_{ow}.2\pi r dr}{\pi R^2} \tag{2-26}$$

390 where u_{ow} is the oil-water flow velocity profile. Again by substituting Eqn. (2-18) into
391 Eqn.(2-26)we have

$$\bar{v} = \frac{1}{\pi R^2}\int_0^R u_\tau \left[2.5ln\frac{(R-r)u_\tau\rho_m}{\mu_m} + 5.5\right]2\pi r dr \tag{2-27}$$

392 Obviously the integration of Eqn. (2-27) is cumbersome to process. However, the
393 equation can be easily integrated by using a computer program such as
394 '*MATHEMATICA*' to obtain a numerical solution as (Kudela, 2010).

$$\bar{v} = \frac{1}{2}u_\tau\left(\frac{2}{k}ln\frac{u_\tau\rho_m R}{\mu_m} + 2B - \frac{3}{k}\right) \approx 2.5u_\tau\, ln\frac{u_\tau\rho_m R}{\mu_m} + 1.75u_\tau \tag{2-28}$$

395 Equation (2-28) shows the relationship between the shear velocity u_τ and the average
396 velocity of the flow droplets $\bar{v}$. Solving Equation (2-28) we obtain a formula relating
397 the shear velocity u_τ to the average velocity of the flow droplets $\bar{v}$ (One exemplary
398 solution is given in the Appendix A),. The value of the shear velocity u_τ of each test
399 point obtained from the average velocity of the flow droplets $\bar{v}$ which are substituted
400 into the Eqn.(2-29) to estimate the mixture flow velocity V_m .Solving Eqn.(2-25) for V_m
401 and let the mixture flow velocity in the water-continuous flow be($V_m = V_{w-m}$):

$$V_{w-m} = \left[\left(\frac{4u_\tau^2 + Dg}{2b}\right).\left(\frac{\rho_m D}{\mu_m}\right)^n\right]^{\frac{1}{2-n}} \tag{2-29}$$

The coefficient b and exponent n can be adjusted to fit friction data better according to the Reynolds number each data in the test matrix. Besides, constant coefficients cannot accurately represent all ranges of turbulent flow (Dong et al., 2016).

2.2 Individual phase flow rate by the drift-flux model

The flow velocities of oil and water phases in oil-water two-phase are different because of the slip existing between the continuous phase and the dispersed phase. So, it is important to estimate each phase flow velocity. However, superficial flow velocities of oil and of water cannot be directly measured downhole. Therefore, it is necessary to have a model of oil-water two-phase which allows allow prediction of these flow rates from flow properties that can be measured in the well(Lucas and Jin, 2001).

The Zuber-Findlay (1965) drift flux model, which was originally develped for gas-liquuid two-phase flow, has been modfied to model the relationship between the oil flow velocity$\left(\frac{V_{so}}{\alpha_o}\right)$ and the mixture flow velocity(V_m) by several authors (Dong et al., 2016; Du et al., 2012; Hasan and Kabir, 1998; Mazza and Suguimoto, 2019). The drift-flux can be express as follows:

$$\frac{V_{so}}{\alpha_o} = C_o V_m + U_{ow} \tag{2-30}$$

where α_o is the oil phase fraction, V_{so} and V_m are the oil superficial velocity, the mixture flow velocity, C_o is the distribution parameter and U_{ow} is the drift velocity of the dispersed phase.

Additional relationships are required for calculating the parameters of the drift-flux model(U_{ow}) and (V_∞). Du et al., (2012), Hasan and Kabir, (1998) and Lucas and Jin (2001) have reported extension of the semi-theoretical correlation of Wallis (Wallis,

1969) to establish a relationship for the drift velocity(U_{ow}) for oil-water two-phaes flow as:

$$U_{ow} = V_{\infty}(1-\alpha_o)^m \quad (2\text{-}31)$$

where V_{∞} is the terminal rise velocity of a single oil droplet of the dispersed phase relative to the continuous phase, α_o is the oil volume fraction and m is the exponent drift velocity model.

Hasan and Kabir, (1998) first suggested for inclined oil–water two phase flow as $m = 2$. In other previous studies, it was suggested that the exponent can be set as $m = 2$ (Du et al., 2012; Lucas and Jin, 2001). In the present study, m is equally selected as 2 for both equations. (2-31) and then use the Harmathy correlation which can be expressed as equation (2-32), (Harmathy, 1960), is often used for calculating the terminal velocityvelocity V_{∞}.

$$V_{\infty} = 1.53\left[g\sigma_{ow}\frac{\rho_w - \rho_o}{{\rho_w}^2}\right]^{1/4} \quad (2\text{-}32)$$

where σ_{ow} is the oil/water interfacial tension, g is the acceleration of gravity.

By substituting the flow parameters -the densities of the water ρ_w 998.4 kg/m^3 and oil ρ_o815 kg/m^3 oil-water surface tension is $\sigma_{ow} = 0.029$ N/m into Eqn. (2-32), the value of $V_{\infty} = 0.131$ (m/s) obtained from the equation(2-32)

It can be seen that in the Eqn. (2-32), the drop size is not included into the expression because of the known fact that under turbulent flow conditions the terminal velocity of liquid particles moving in liquid media is practically independent of the particle size(Harmathy, 1960).

To determine the value of the distribution parameter C_o, we substitute, V_∞, V_{so}, V_m and α_o into Eqn. (2-30) for expressing the general drift-flux equation as:

$$\frac{V_{so}}{\alpha_o(1-\alpha_o)^2} = C_0 * \frac{V_m}{(1-\alpha_o)^2} + V_\infty \quad (2\text{-}33)$$

The volumetric flow rates of oil (Q_o) and water (Q_w) flowing into the working section were measured at the inlets with the single phase flow meters. The reference superficial velocities of oil and of water were obtained the single phase flow rate using the expression $V_{so} = (Q_o/A_p)$ and $V_{sw} = (Q_w/A_p)$ respectively. The reference mixture flow velocity is the sum of the two superficial velocities, $V_m = V_{sw} + V_{so}$. The mean volume fraction α_o of the oil in the working section was determined from the gamma densitometer measurements. The distribution parameter (C_0), can be estimated by plotting the quantity $V_{so}/\alpha_o(1-\alpha_o)^2$ against $V_m/(1-\alpha_o)^2$ as it would be expected from equation (2-33)that the data would fall on a straight line with slope $C_0 = 1.1$ and intercept $V_\infty = 0.131$ as shown in Figure 2-3.

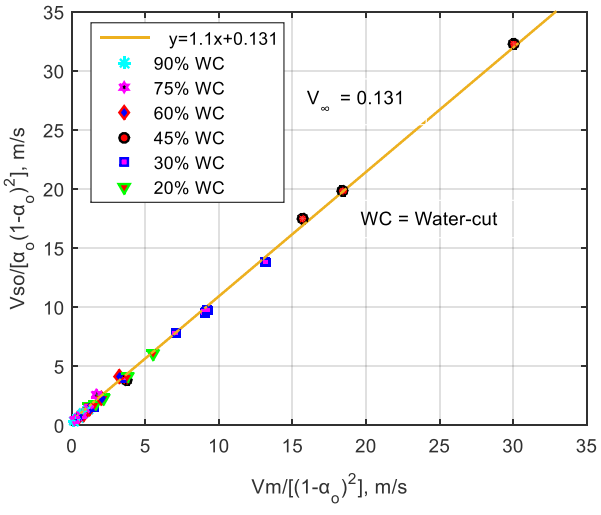


Figure 2-3 $V_{so}/\alpha_o(1-\alpha_o)^2$ versus $V_m/(1-\alpha_o)^2$ for vertical upward flow.

This is in a good agreement with the value of the distribution parameter reported in the literatures (Hasan and Kabir, 1998; Picchi et al., 2015).

The estimated mixture flow velocity of either the oil-continuous flow or the water-continuous flow can be used to predict the the superficial velocity of oil and of water as follows:

$$V_{so} = \alpha_o[C_o V_m + U_{ow}] \tag{2-34}$$

$$V_{sw} = V_m - V_{so} \tag{2-35}$$

2.3 Overall estimation procedure

A schematic diagram of the measurement concept for two-phase oil-in-water flow is illustrated in Figure 2-4. The CWDU flow sensor estimate the average velocity of the droplets (dispersed phase) using Eqn. (2-1). The gamma-ray densitometer was used for measuring the phase fraction of oil in the mixture flow, and subsequently, the mixture density is calculated using equations (2-9) and (2-24) respectively. For oil continuous flow, the velocity profile follows the behaviour of laminar flow and the mean flow velocity can be estimated based on the equation (2-16). Whereas, for the water-continuous flow which has turbulent velocity profile, the flow velocity is estimation by substituting the values of the mixture density, viscosity, shear velocity, pipe diameter and acceleration due to gravity into Eqn. (2-29). Subsequently, the drift-flux model is applied to calculate the individual phase velocities from the overall flow velocity and the phase fraction estimates with Eq. (2-34) and (2-35).

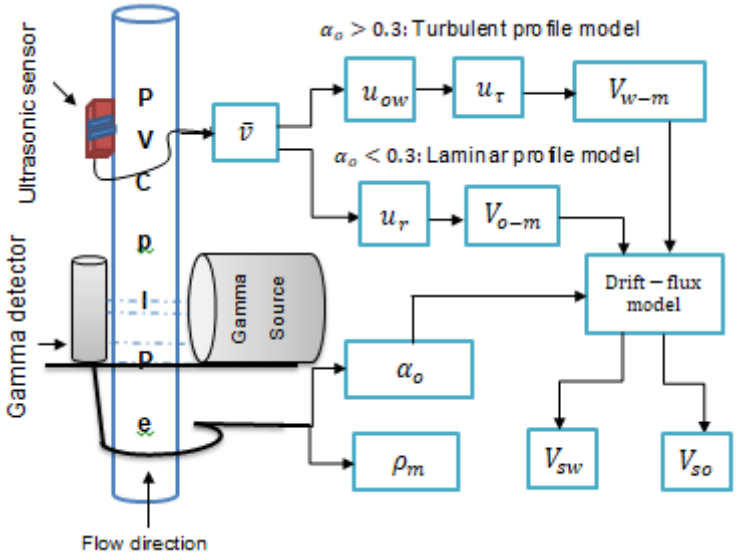


Figure 2-4 Combined systems of the CWDU sensor and gamma densitometer for measurement of two-phase oil-water flow

3 Experimental setup

3.1 Flow facility, apparatus and test fluids

The experimental investigations to measure vertical up flow of oil-water two-phase flow were conducted in a multiphase flow test rig at Cranfield University, Bedfordshire, United Kingdom. Figure 3-1 shows a schematic representation of the multiphase flow test rig. The flow facility consists of the test rig, water tank, oil tank, a separator, two centrifugal pumps and measuring equipment. The experimental pipeline is a 2" schedule 10 stainless steel pipeline consisted of an entry length of 40.0m long horizontal and 10.5 m high vertical to ensure enough development length is allowed for the flow. A transparent PVC pipe test section of 1.2 m long and 50. 8 mm i.d. is provided for clear observation of the flow phenomena at approximately 8.5 from the riser base. At the exit of the test section, there is a pipe length of 0.60 m to avoid any flow disturbance in the test section.

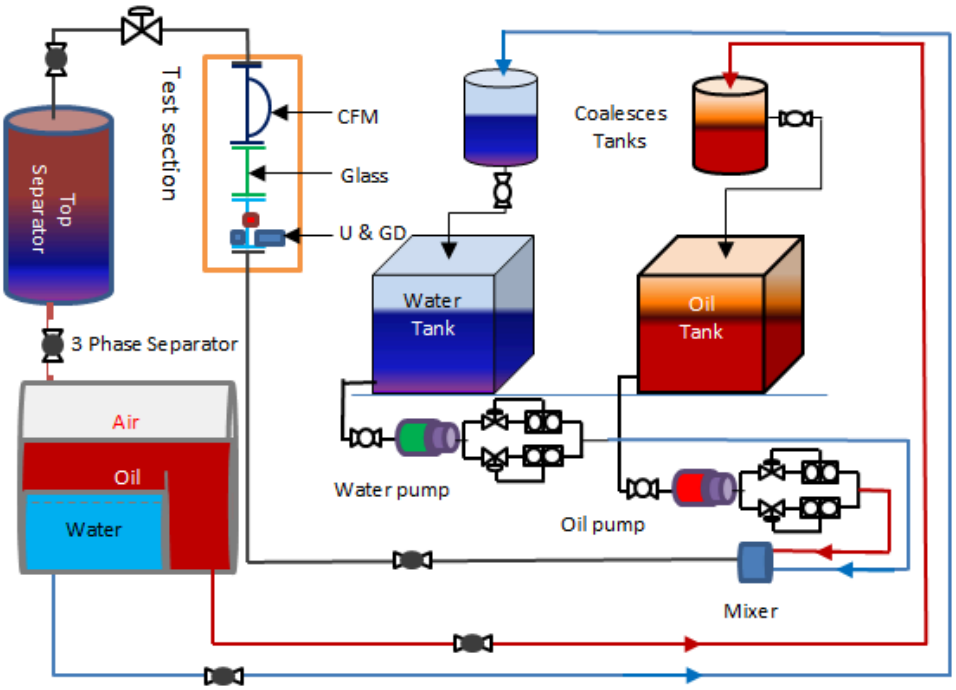


Figure 3-1 Schematic diagram of the test facility

3.2 Experimental procedure

Process management software (Emerson DeltaV) provided digital automation to the operation of the test rig (process plant) which allowed for setting the input water and oil flow rates, and selection of the appropriate pumps and flowmeters. Two separate dedicated PCs, one with a LabVIEW® for the CWDU sensor and the other with Chastotomer® software for the gamma densitometer are used for the data acquisitions. In addition to the two PCs for measurement systems, another PC with LabVIEW software program is used for recording all the data from the reference instruments. The test fluids used in the experiments are tap water (density of 998.4 kg/m^{3}and viscosity of 0.001Pa.s at at 21℃) and dyed mineral-dielectric oil (Rustlick EDM-250, density of 815kg/m^3 and a viscosity of about 7.2mPa at 21℃). The oil flow and water flow were pumped individually from their storage tanks (12.5 m^3 capacity) into the rig pipeline through a Y-mixer-manifold, first into the horizontal pipe and then flowed up to the

506 vertical pipe section. The oil flow was metered by the reference Micro Motion Mass
507 flowmeter and a Foxboro Coriolis meter while the water flow was metered by the
508 reference a Rosemount flowmeter and a Foxboro CFT50 Coriolis meter before the two
509 liquids were mixed prior to the test section.
510 A Coriolis mass flowmeter (Endress and Hauser Promass 83F) was installed at top of
511 the test section at approximately 11.0 m from the riser base to measure the oil-water
512 mixture mass flow and density as a reference density meter. All the reference
513 flowmeters were, prior to the experimental study, calibrated against a primary reference.
514 The specifications and operating ranges of the reference flowmeters are given in Table
515 1.
516 Table 2 Details of instruments of the flow rig

Instruments	Items	Manufacturer	Model	Range	Error (of the span)
Coriolis Flowmeter	Oil flow	Micro Motion	F200	up to 1.0 kg/s	±0.2%
Coriolis Flowmeter	Oil flow	Foxboro	CFT50	up to 10.0 kg/s	±0.10%
Coriolis Flowmeter	Water flow	Foxboro	CFT50	up to 10.0 kg/s	±0.10%
EM Flowmeter	Water flow	Rosemount	8742C	up to 1.0 kg/s	±0.5%
Coriolis Flowmeter	Mixture flow	Endress and Hauser	Promass 83F	0 to 50.0 kg/s	±0.10%

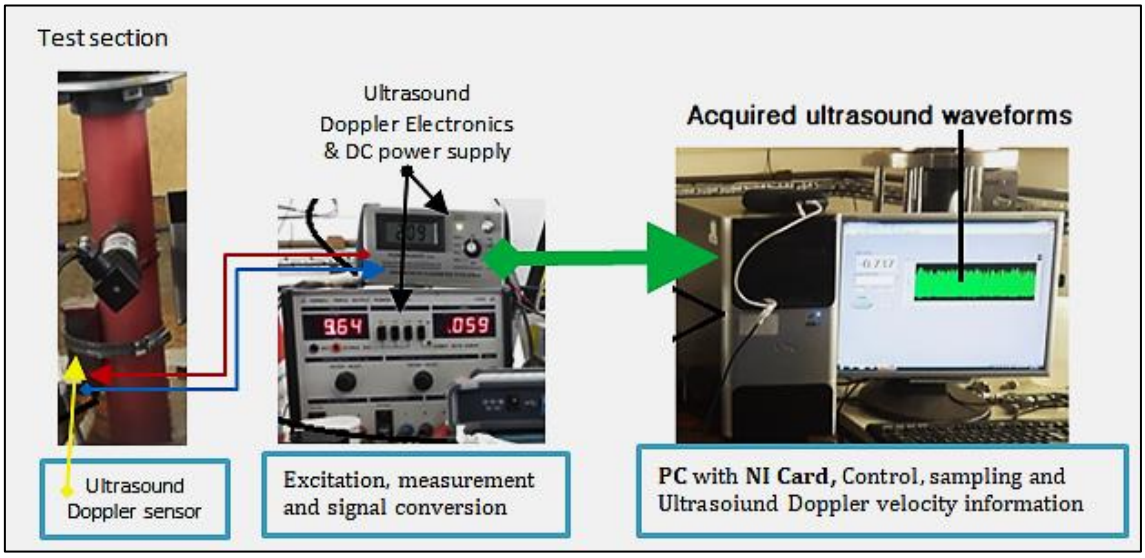


Figure 3-2 Oil-water flow test section showing the CWDU sensor set up

The water cut is defined as the ratio between the water and total volumetric flow rates as introduced to the inlet section (Ibarra et al., 2017). The flow velocities at the inlet of the rig were calculated as: superficial velocity of the water flow $V_{sw} = Q_w/\rho_w A_p$ and the oil superficial velocity $V_{so} = Q_o/\rho_o A_p$ with A_p being the cross-sectional area of the pipe, $A_p = \pi D^2/4$. The flow rates are varied from 0.28 kg/s to 2.78 kg/s ($1\text{m}^3/\text{h}$ to $10\ \text{m}^3/\text{h}$). For each experimental run, the inlet water cut, WC, was varied between 20% and 90% while the total flow velocity, V_m, was kept constant. Surely, this creates two categories of flow: water-dominated flow or oil-dominated flow. However, the drift velocity model can be applied to either status of the continuous phase. This is because the terminal rise velocity of a single droplet of the disperse phase is relative to the continuous phase(Lucas and Jin, 2001). Importantly, the variation of the water-cut has allowed us to observe of flow velocity measurements while the water cut being changed at constant total flow velocity.

A wide range of flow rates for mixture flow at different water-cut were measured to collect a maximum amount data. The test matrix of the data is shown in Figure 3-3. All test runs were performed at near atmospheric pressure and at a temperature of 21 ± 2 °C. After the mixture flows pass through the test section, it then entered into the separation equipment which comprises gravity separators and coalesce-tanks. The mixture flow undergoes separation process and then flow flowed directly into their respective storage tanks after for re-use.

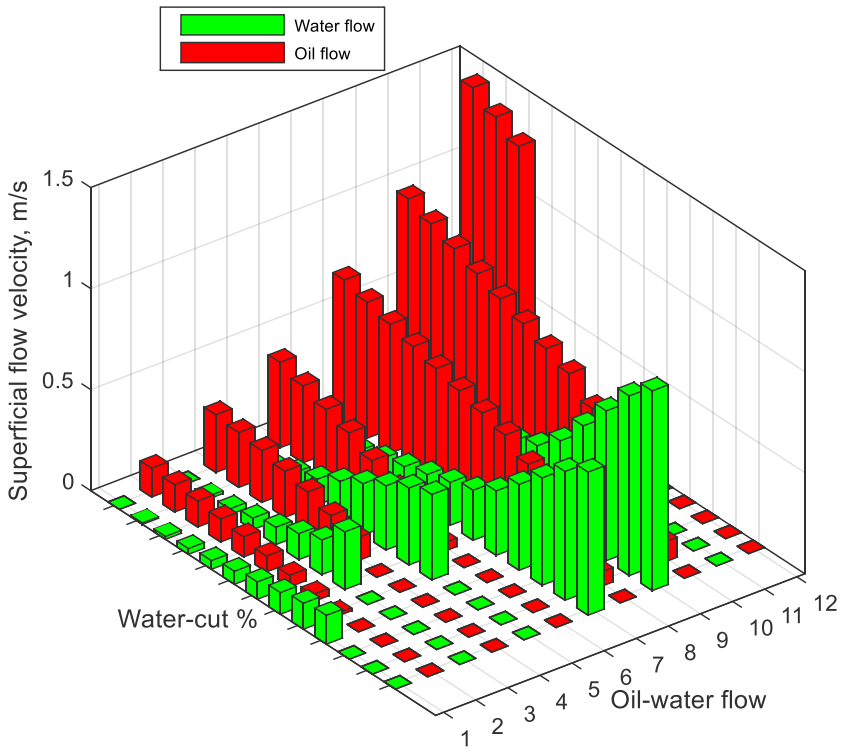


Figure 3-3 Graphical illustration of the test matrix

3.3 CWDU flow sensor instrumentation

The ultrasonic Doppler flow sensor (United Automation Ltd, Southport, UK) has 0.5-MHz centre frequency and contains a co-housed two piezoelectric chips (*viz*: T and R) T is for transmitting of ultrasonic waves into the flow and the R for receiving the signals from the scatterers. Therefore, the measurement volume of the present CWDU sensor has a square-shape determined by the effective diameters (20mm×20mm) of each

element. The sensor was bounded onto the side of the test section pipe using a clip and a gel to give a firm grip and better contact between the senor and pipe wall and then it was connected to a signal conditioning electronic circuit which provided both the excitation voltage of the transmitting Doppler piezoelectric chip and facilitation of the data acquisition.

In the present study, the excitation voltages of the transmitting Doppler flow meter sensor were +18v and -18v (36v peak-peak). Table 2 shows the material used in the experiments and their related acoustic velocity. Figure 3-4 shows a schematic CWDU sensor system

Table 3 physical properties of the material considered

Material	Speed of sound (m/s)	Density (kg/m^3)
Water (20℃)	1484	998.4
Oil (20 ℃)	1324	815.4
PVC	2380	1380
Stainless steel	5790	7890

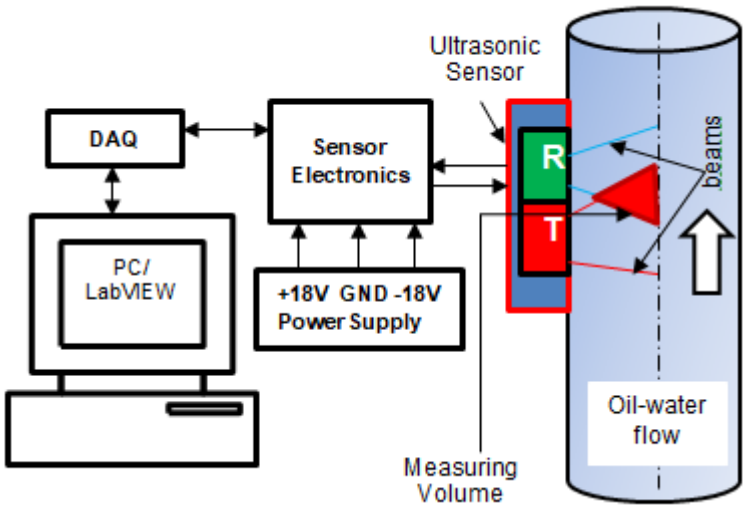


Figure 3-4 a schematic diagram of the CWDU sensor system

The Doppler signals were recorded continuously for 20 s at a sampling frequency of 10 kHz which is long enough for the flow regime profile to pass through the test section (Zhai et al., 2013). The recorded signal was passed through an anti-aliasing filter and digitized using a computer-based ADC card (Nl E-series card PCI-MIO-16E-4, National Instruments, Austin, TX, USA), and recorded onto a hard drive of a PC. The entire data acquisition process is controlled using graphical programming language LabVIEW 10 software.

The recorded Doppler signal was processed off-line using MATLAB (The Math Works, Natick, MA, USA) on a Widows 7 workstation) for obtaining the mean frequency shifts using an intensity-weighted-mean(IWM) equation(Morriss and Hill, 1991). The flow velocity is calculated using the estimated mean frequency shifts and the sound speed in the fluid. The literature values used as the sound speed and density were 1484 ms^{-1} and 998.4 kg/m3 for water respectively and corresponding values in the oil were 1324 $ms^{-1}$and 815.4 kg/m3 respectively(Onda, 2003).

Many techniques exist to compute the Doppler spectrum efficiently, based on FFT for example. Liu et al., (2021) reported an application of the FFT algorithm for Doppler spectrum of oil-water flow ultrasound Doppler for flow pattern identification and the authors also demonstrated that the non-invasive CWDU sensor is suitable for both flow velocity measurement and flow patterns identification.. In In the present study, the digital signal processing of the ultrasound Doppler signal consists of two parts: fast Fourier transform (FFT) algorithm and intensity weighted mean (IWM) estimation. Firstly, the data series is decomposed into a series of signal in the form of framed with the powers of 2 and windowing to evaluate the frequency spectrum. The windowing

technique prevented unwanted frequency appearing in the spectrum. Secondly, with the FFT, the spectrogram yield instantaneous frequencies as functions of time that give sharp higher amplitude for the signal reflected off the droplets(Case et al., 2013).

Figure 3-5 and Figure **3-6** are taken from the test data points and they show the logged raw ultrasonic signal and its Doppler spectrogram calculated using short time Fourier transform(STFT). The STFT plot or the spectrogram displays distribution of the frequency shifts in the oil-water two-phase flow. In the case of Figure 3-6, the spectrogram displays signal strength by colour intensity. Doppler shift frequency is relatively low and in the present study it ranges between 60Hz and 800Hz and the low frequency components in the spectrogram are not noise. So, they will not affect the measurement results.

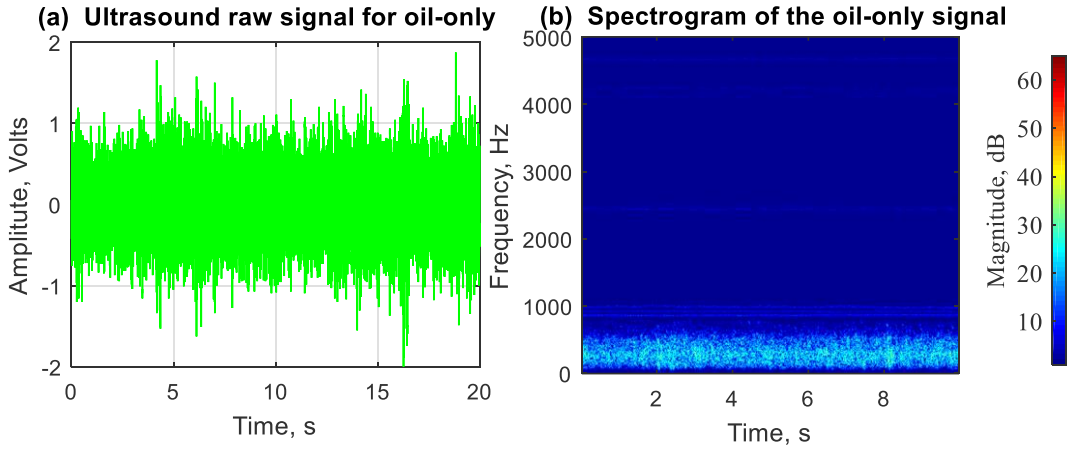


Figure 3-5 Example of the continuous wave ultrasound signal and its: (a) Raw signal, and (b) STFT, for conditions*:* Vm = 1.25 m/s, WC = 0%, and a 10kHz signal acquisition frequency.

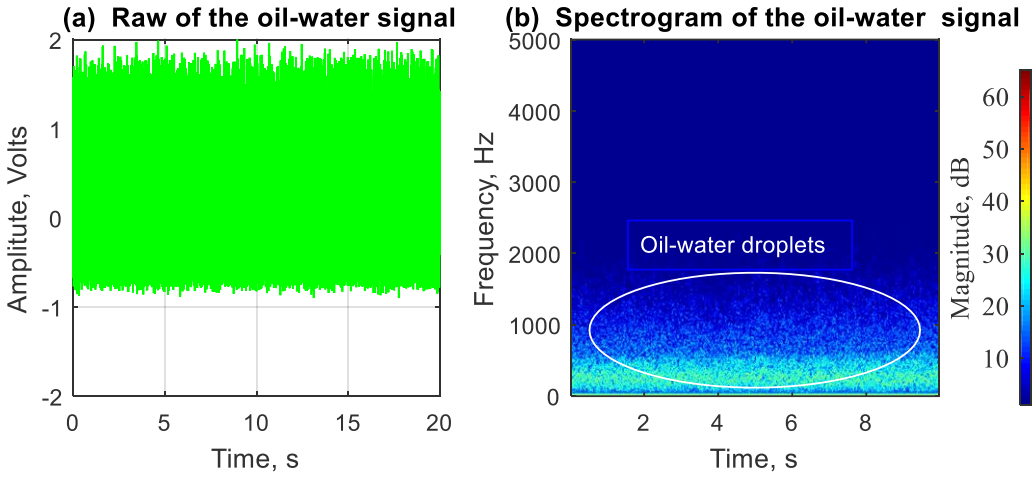


Figure 3-6 Example of the continuous wave ultrasound signal and its: (a) Raw signal, and (b) STFT, for conditions: Vm = 1.25 m/s, WC = 60%, and a 10-kHz signal acquisition frequency.

3.4 Gamma densitometer system

The gamma densitometer used in this study employs Caesium-137 isotope. The gamma source, detector and a data processing unit are manufactured by the Neftemer® Ltd as a clamp-on multiphase flowmeter. The gamma source housing provides an outlet that produces a cone of beam six degree wide having uniform physical properties directed across the pipe diameter. The caesium-137 isotope emits 0.1 – 0.94 MeV photon energies. The detector unit comprises scintillation crystals (NaI), photomultiplier tube (PMT), amplifier electronics and single channel analyser (SCA) and a temperature control. The PMT contains photocathode and focussing electrodes. The scintillation crystals produce a pulse of visible light with energy proportional to that of the incident gamma photon and are detected by the photocathode which produces electrons by photoelectric effect. The amount of the electrons by the photocathode is low and it has to be amplified by the photomultiplier which converts the light pulses into voltage pulses of proportional amplitudes. The voltage pulses undergo signal conditioning then

passed on to channel analysers for classification(Kumara et al., 2010a; Tesi, 2011).The scattering of the gamma electromagnetic radiation by the matter via interaction of the photons with the matter can take several forms but the two methods of photoelectric or Compton scattering are the most frequency used at low energy emissions (Kumara et al., 2010a). The photoelectric type is the one used in the present study.

The gamma-source and detector are arranged diametrically opposite to each other with the gamma densitometer source emitting a narrow beam of radiation and an opposing detector scan across the pipe-section for measuring the average flow volume fraction across the whole pipe diameter(Kumara et al., 2010a). Figure 3-7 shows the schematic diagram of the gamma densitometer instrumentation set up in which the variables I_0 and I are the incident and the received intensities of the gamma-rays.

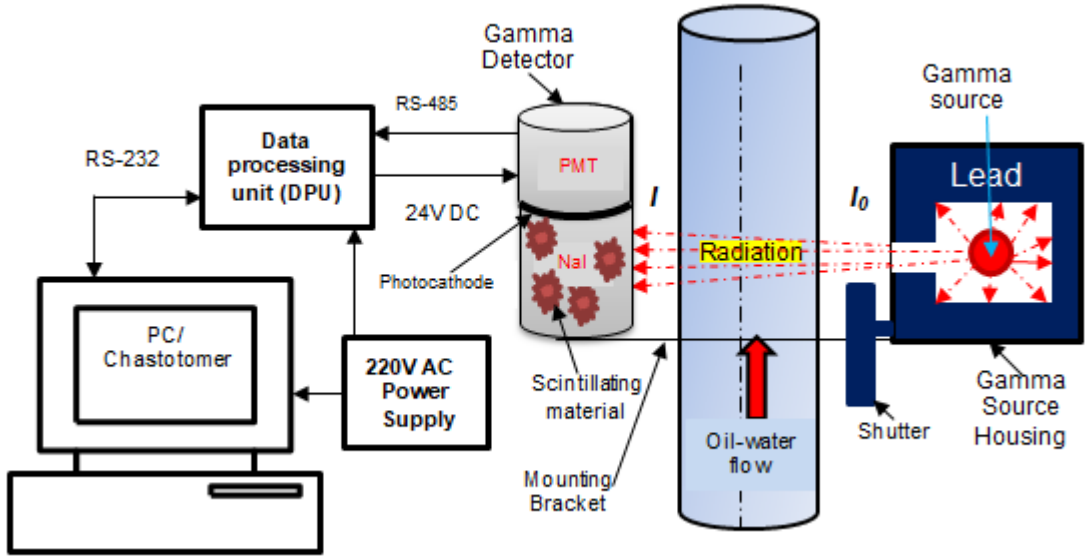


Figure 3-7 Schematic diagram of a single-beam gamma densitometer system

Single phase flow calibration is required for the determination of the volume fractions at the beginning of every test point (Falcone et al., 2009). Therefore, the gamma count rates of single phase water flow I_w and of oil flow I_o were obtained and recorded. The

data is collected every test point and then stored for further processing. The flow parameters such as phase fraction and the mixture density can be calculated from the average pulse count rate and the calibration results (Falcone et al., 2009; Kumara et al., 2010a)

Figure 3-8 shows Examples of the gamma densitometer counts from (a) oil only signal, and (b) oil-water signal, for conditions overall velocity *Vm* = 1.25 m/s, WC =60%. A sampling at 250 Hz frequency was used and a total of 75,000 samples (which corresponds to 300 s sampling time (5 minutes) were collected at each sampling point.

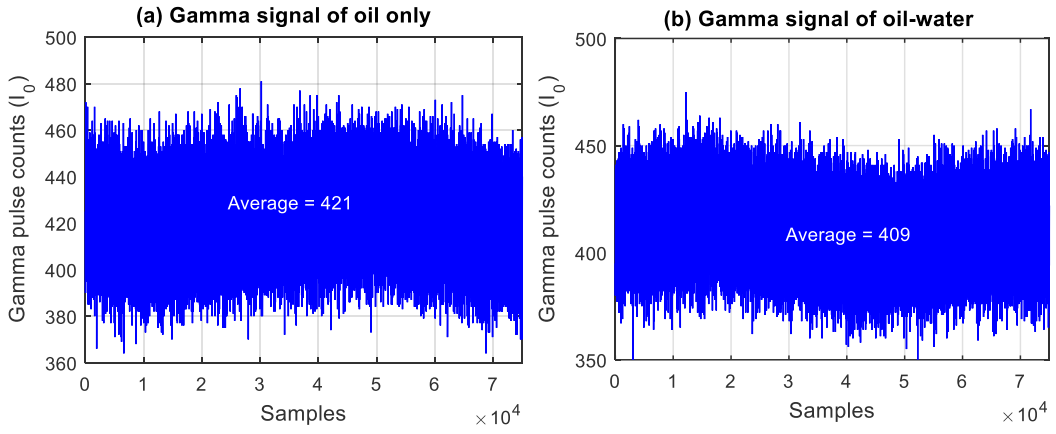


Figure 3-9 Gamma-ray densitometer pulse counts obtained from (a) Oil only signal, and ((b) oil-water signal

3.5 Experimental observation

From the observation of these experiments, vertical upwards oil/water flows, it was evident that when the flow velocities were relatively high (e.g. the mixture velocity above 0.60 m/s), the oil and water were well mixed and the flow regime was a dispersed flow. When the mixture velocity was low, then the flow regime was churn flow. This observation is also consistent with the recommended criteria for discriminating dispersed and non-dispersed oil/water upwards flows by API, (2015). More detailed flow regime classifications were reported by other published studies.

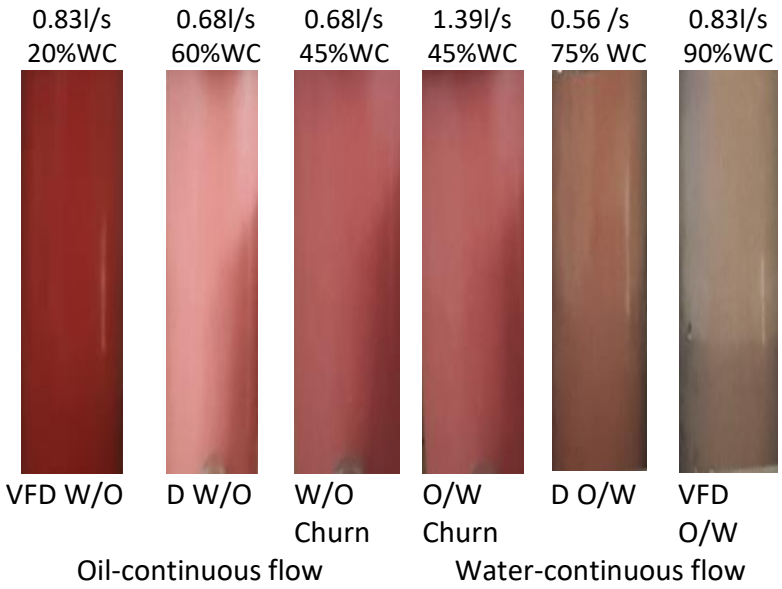
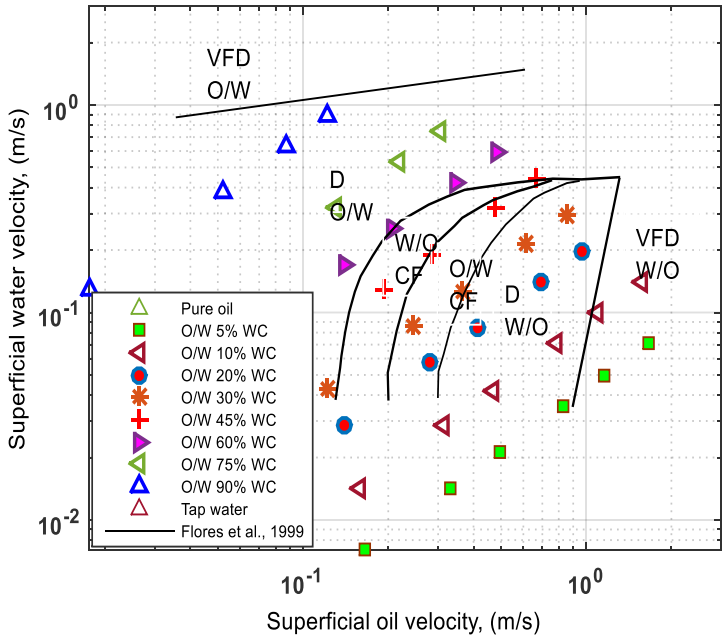


Figure 3-10 Photos of the flow pictures taken in the experiments

Flores et al., (1999) conducted experimental investigation for characterization of vertical oil-water flow and defined the flow patterns in oil-water two-phase vertical flow into six flow patterns belonging to two dominant classes: *oil-continuous flow* (water in oil churn flow, dispersion water in oil, and very fine dispersion water in oil), and *water-continuous flow* (oil in water churn flow, dispersion oil in water, and very fine dispersion oil in water). in the present study, the oil-water upward vertical flow map produced by Flores et al. (1999) was used to map the flow data as shown in Figure 3-11. Furthermore, we developed the flow measurement model that allows study of the oil-water two-phase flow based on (1) the oil continuous flow, flow and (2) the water continuous flow, and to predict the superficial flow velocity of the oil and water by using established drift-flux model. These two main flow patterns were expected to occur in oil-water two-phase flow according to some authors (Dong et al., 2016, 2015; Lovick and Angeli, 2004).



669

670 **Figure 3-11** the experimental test points plotted on the transition map by Flores et al.,
671 (Flores et al., 1999)

672 ## 3.6 Reynolds number of the oil-water two-phase flow

673 The Reynolds number(Re), is the ratio of inertial forces to viscous forces acting on a
674 fluid. For a circular pipe is laminar for Re $\leq$ 2300, turbulent for Re $\geq$ 4000, and in
675 between them is transitional. Reynolds number of the oil-water two-phase flow
676 investigated in the present study was plotted against the input flow volume water
677 fraction. Figure 3-12 shows a plot of Reynolds number of the oil-water two-phase
678 mixture flow velocity range from 0.14 m/s to 1 m/s and the input water cut from 0% to
679 100%. The plot is used for classification of the flow velocity profiles. The Reynolds
680 number *Re* for two-phase flow is defined as:

$$Re = \frac{Inertial\ forces}{Viscous\ forces} = \frac{\rho_m V_m D}{\mu_m} \tag{3-1}$$

681 where μ_m is the dynamic viscosity of the two-phase flow and V_m is the mixture flow
682 velocity.

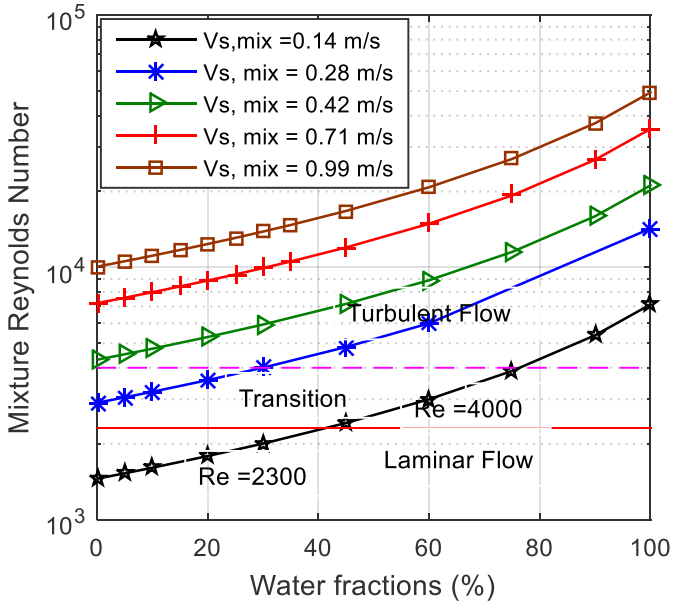


Figure 3-12 Mixture flow Reynolds number as function of water fraction

4 Results and discussion

4.1 Mixture density measurement

Using the non-invasive capability of the gamma-ray densitometer, the density of the mixture flow and the oil volume fraction investigated in these experiments were measured. Figure 4-1 shows mixture densities obtained from the measurements with gamma-ray densitometer compared with the reference Coriolis flowmeter. From the Figure 4-1, it can be seen that the difference between the densitometer measurements and the reference mixture density rose up to $\pm 13\%$ at $1 m^3/hr$ and then fell down to less than $\pm 5\%$ at $6 m^3/hr$. So, in oil-water two phase flows, the measurement of the mixture flow density is affected by the flow rate.

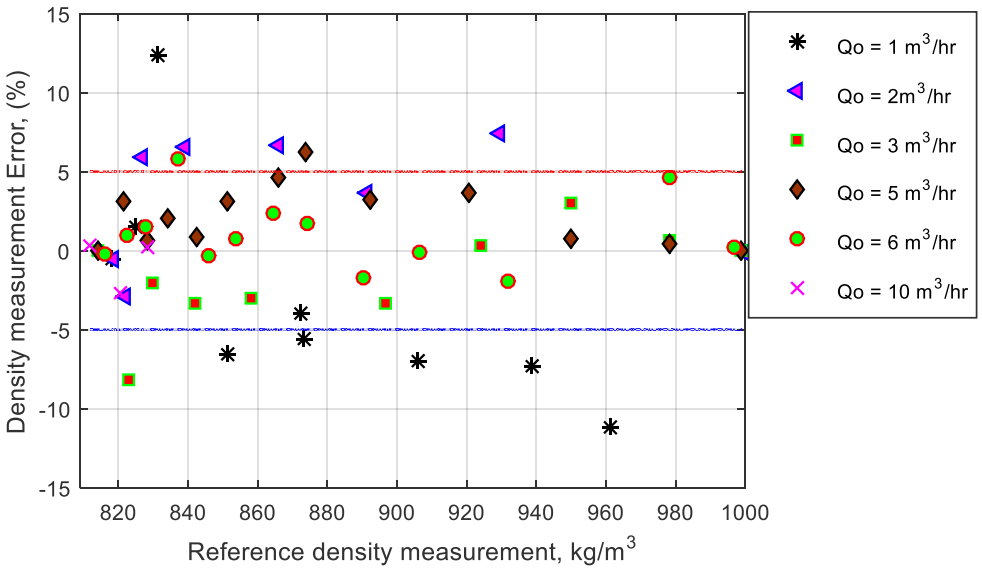


Figure 4-1 The relative errors of the mixture flow density

4.2 Mixture flow velocity measurement.

The oil-water two-phase flow is considered as a water-continuous flow when the inlet water-cut is greater than or equal to 30%. Otherwise, it is considered as an oil-continuous flow(Brauner and Ullmann, 2002; Dong et al., 2016). The mixture mean flow velocities were computed from the measured local velocities in the measuring volume and the flow veloity profile models through the applying equations (2-16) and (2-29). The results are shown in Figure 4-2 and Figure 4-3 for the oil-continuous flow and for water-continuous flow respectively.

The relative error and the absolute error for the flow measurement results are calculated using (4-1)and (4-2) respectively.

$$\mathrm{E_r} = \frac{\mathrm{Data_{est}} - \mathrm{Data_{ref}}}{Data_{\mathrm{ref}}} \times 100\% \tag{4-1}$$

where $\mathrm{Data_{est}}$ is the estimated result in oilr-continuous flow (V_{o-m}) and water-continuous flow$(V_{w-m})$and $\mathrm{Data_{ref}}$ is the reference mixture flow rate measured by the single phase flowmeters. The average absolute of the error is:

$$\varepsilon_{ave} = 1/N_s \sum |E_r| \quad (4\text{-}2)$$

where N_s is the sample number.

4.2.1 Oil-continuous flow

Comparison between the estimated mixture flow velocity predicted by equation (2-16) and the total mixture flow velocity obtained by the flow rates at the inlets is presented in Figure 4-2. For evaluating the accuracy of the proposed model, calculated both the relative error and the absolute error of the results. It can be seen that at most test points, the relative error (E_r) is within ± 8.0 % of the reference mixture flow velocity. This agreement is considered quite good considering the statistical nature of the experiments and the oil-water flow phenomena.

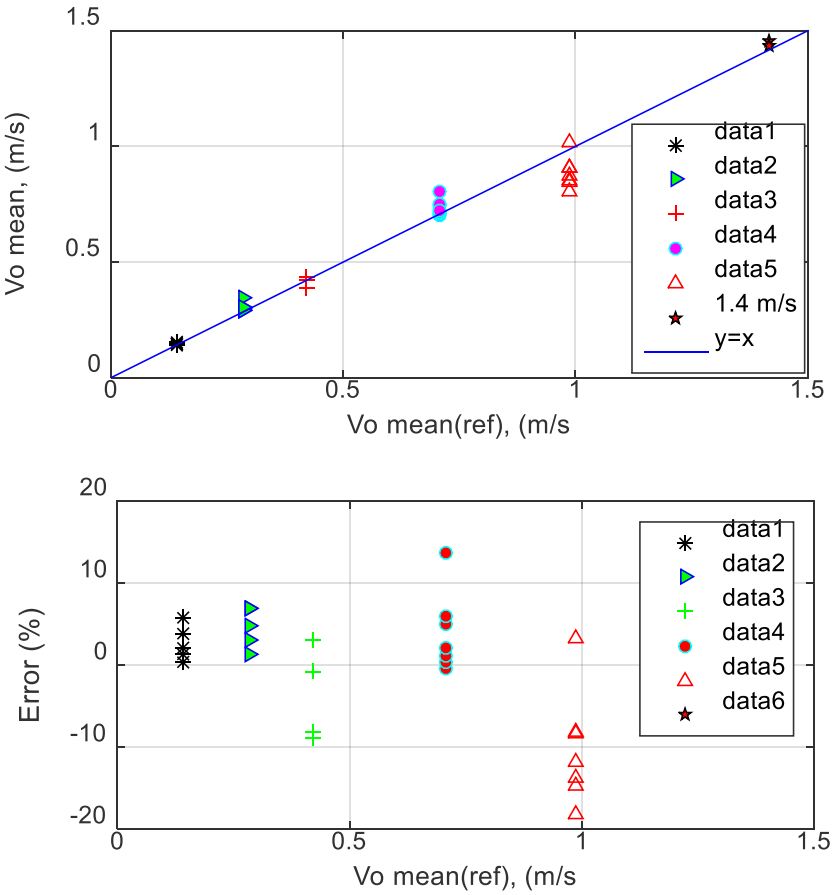


Figure 4-2 Measurement mean velocity of oil-continuous flow in oil-water two-phase flow

Finally, the mixture superficial velocity of oil-continuous flow was predicted by the equation (2-16) and the results show that the mean relative error was equal to 5.2% and maximum relative error was equal to 17.6%.

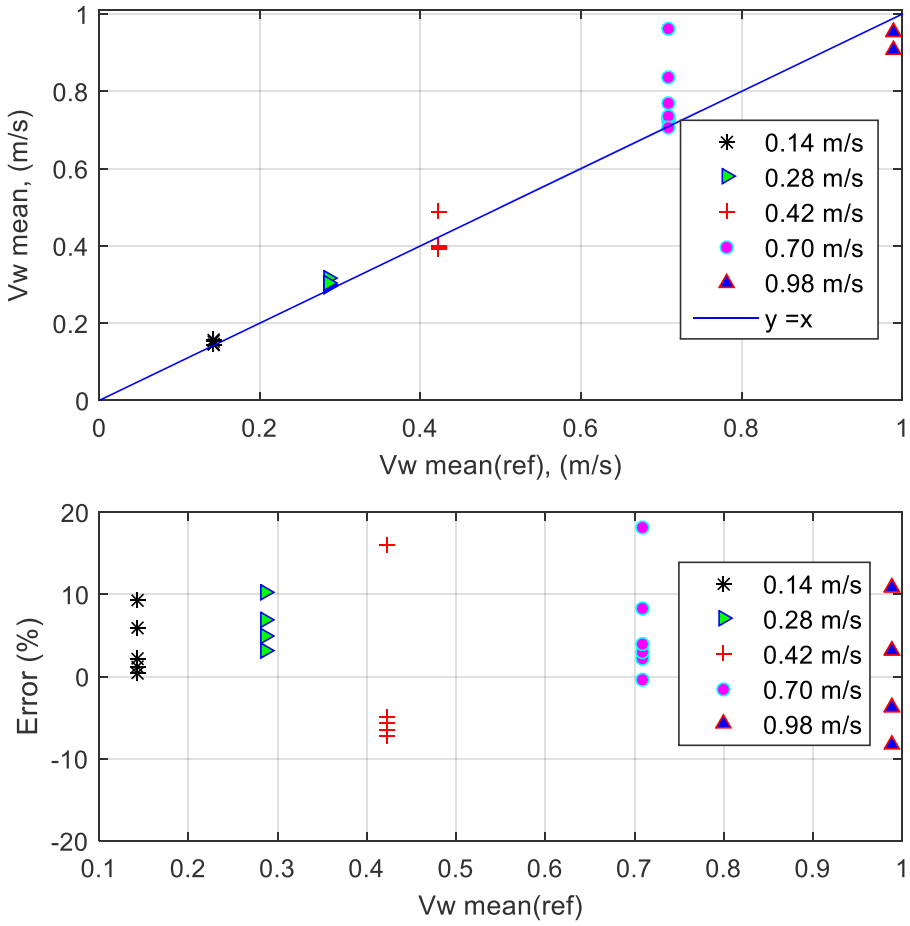
4.2.2 Water-continuous flow

The mean superficial velocity of the water-continuous flow can be estimated using the measured flow velocity in the measuring volume and corrections to account velocity profile in the pipe. The water-continuous in the present experimental set-up can be estimated using equation (2-29). The results for the water-continuous flow model were similar to the oil-continuous flow model. Figure 4-3 show the results from the water-continuous flow model.

For the Eqn.(2-29), the friction factor's coefficient b and exponent n are to be determined for estimating the mixture flow velocity. There are many experimental data for these two coefficients in the literature. For an example, Blasius correlation for a tube with a smooth wall and for 2000 < Re <10^5 set the values of the coefficient b and exponent n as 0.316 and 0.25 (Descamps et al., 2006). In addition, the values of the coefficients b and n presented by Bannwart (Bannwart, 2001) for the Reynolds number range of the 2×10^3 to 10^5 range between 0.19 to 0.443 and 0.19 to 0.28 respecively. In the present experiment, selection of the coefficient b and exponent n were obtained by using the Blasius correlation as a benchmark and then the flow velocity predictions were turned to best fit fit for each flow velocity. the Blasius correlation($b = 0.316$ and exponent$n = 0.25$) equivalent values in the present study are as shown in Table 4.

Table 4 Friction factor coefficients

Mixture flow velocity, m/s		Present experiment predicted values of coefficient b and exponent n	
1.	0.143	b = 8.0;	n = 0.008
2.	0.285	b = 4;	n = 0.06
3.	0.423	b = 2;	n = 0.07
4.	0.708	b = 0.80;	n = 0.06
5.	0.988	b = 0.316;	n = 0.025



745

746 **Figure 4-3** Measurement mean velocity of water-continuous flow in oil-water two-

747 phase flow

As illustrated in Figure 4-3, the mixture flow velocities estimated when the flow condition is water-continuous flow-mean relative error was equal to 2.8% and maximum relative error was equal to 17%.

Moreover, in comparison with the horizontal oil-water two-phase measurement using CWDU flow sensor method by (Dong et al., 2015) with the present experiment, the mixture flow velocity estimated in water-continuous flow maximum relative error was equal to 11.8% and mean error 3.11% while the oil-continuous flow conditions has maximum relative error 12.2% and mean relative error 4.8% respectively. This suggests that the present study conducted on a vertical flow pipe good non-invasive flow measurement system can readily be achieved with using the ultrasound Doppler method.

4.3 Effect of water-cut on mixture flow velocity

The mixture velocities are evaluated for various input water-cut and these measurements result are then compared to the reference to experimental results. Figure shows that 87% points measured values are well within $\pm$10% and 56% points are within $\pm$5%. The errors in the measured mixture flow densities for the different volume fraction were was due to the flow structure changes even at constant the total mixture flow rate.

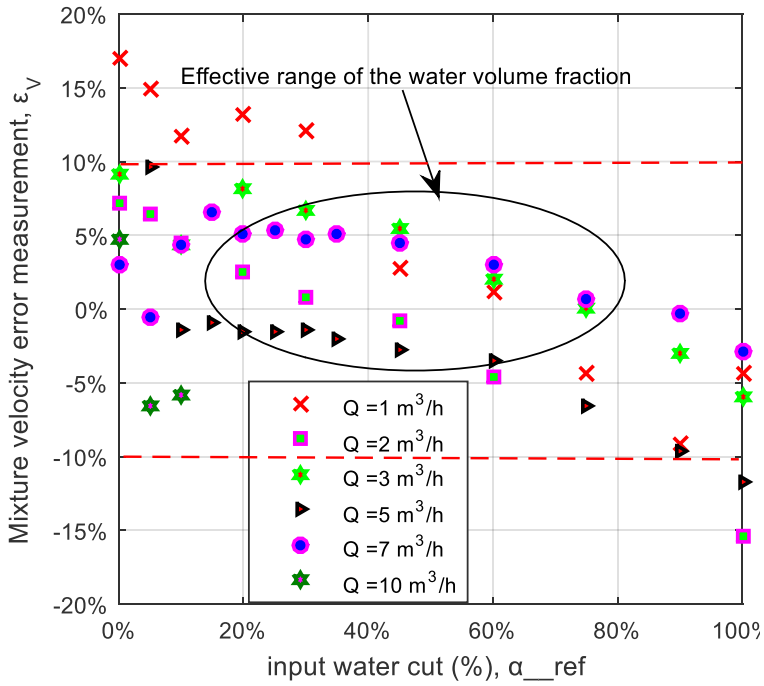


Figure 4-4 Measured mixture flow velocity in varied water volume fractions

4.4 Prediction of the superficial velocities of the oil and the water

The oil-water mixture flow velocity in both oil-continuous flow and water-continuous flow can be determined using the CWDU method proposed in this study. However, the superficial velocities of the oil and the water are frequently required to be determined(Lucas and Jin, 2001). The individual phase superficial velocities of oil and of water were estimated using the drift-flux model in which the mixture flow velocity and phase fraction are the inputs. The results were compared with single phase flowmeter measurement at the flow inlets prior to the mixing.

Equations (2-34) and (2-35) were used for the calculation of superficial flow velocity of oil and of water respectively and the initial results showed slight underestimation and overestimation. Hence, correction factors are essential to modify both Eqns.(2-34) and (2-35). Since the original results obtained from using the equations (2-34) and (2-35)were linear, consequently, the two equations were corrected individually using

781 determined by using a least-squares method based on linear portions of the original
782 estimates. These yielded the equations which resulted in in Eqns. (4-3) and (4-4) for the
783 superficial flow velocity of oil and water respectively, as:

$$V_{so-mean} = 0.78 * V_{so} \tag{4-3}$$

784 and

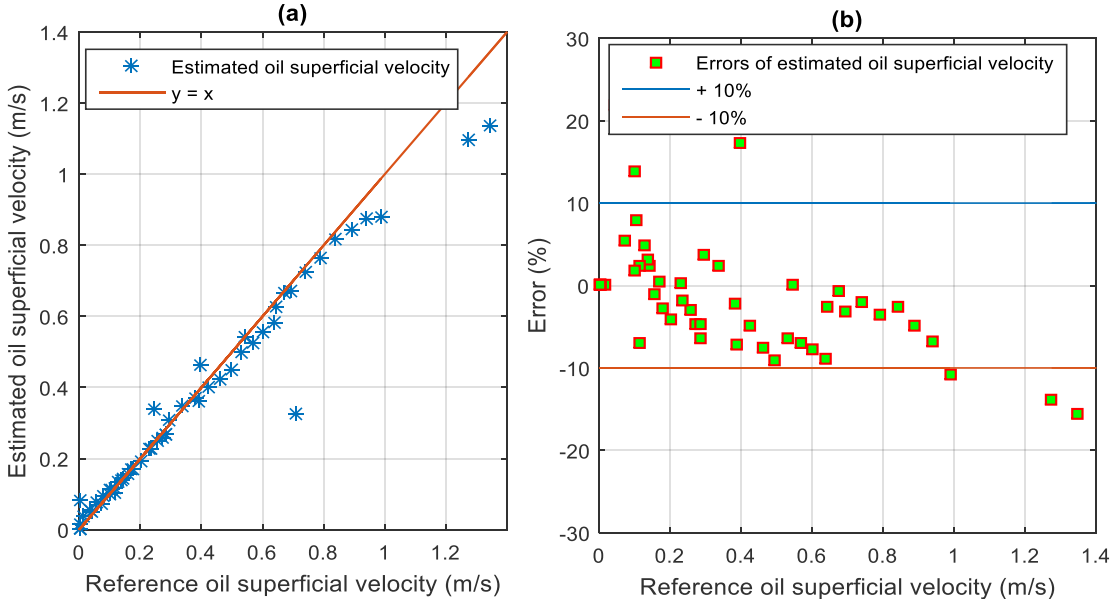
$$V_{sw-mean} = 1.08 * V_{sw} \tag{4-4}$$

785 Figure 4-5 shows the results for estimation of superficial velocity of oil using the
786 equation (4-3). Similarly, Figure 4-6 shows the results of using Eqn. (4-4) for water
787 superficial flow velocity respectively. The superficial phase flow velocity of oil is $\boldsymbol{V_{so_i}}$,
788 and $\boldsymbol{V_{R,so_i}}$ as the reference value. The relative error $\boldsymbol{\delta_i}$ is defined as:

$$\delta_i = \frac{V_{so_i} - V_{R,so_i}}{V_{R,so_i}} \times 100\% \tag{4-5}$$

789 where $\boldsymbol{i}$ is the test point number, and the average relative error can be expressed as:

$$\overline{\boldsymbol{\delta_{Vso}}} = \frac{\boldsymbol{1}}{\boldsymbol{N}} \sum_{\boldsymbol{i=1}}^{\boldsymbol{N}} |\boldsymbol{\delta_i}| \tag{4-6}$$



790

Figure 4-5 (a) the predicted superficial velocity of oil by equation (4-3) versus the reference superficial velocity of oil (b) The percentage error in superficial velocity of oil versus the reference superficial velocity of oil

Figure 4-5 illustrates the comparison of the estimated superficial flow velocity of oil obtained from equation (4-3) plotted against the reference oil superficial velocity. It was observed that the average relative error $\boldsymbol{\delta_{Vso}}$ was equal to 4.5% and the maximum relative error was equal to 19.15%.

Using two equations similar to equations (4-5) and (4-6)the percentage error in the predicted water superficial velocity $\mathbf{V_{sw}}$ be calculated for each test point. Figure 4-6 illustrates the comparison of the estimated water phase flow velocity obtained from equation (4-4) plotted against the reference water superficial velocity. Again, it was also observed that the average relative error $\boldsymbol{\delta_{Vso}}$ was equal to5.98% and the maximum relative error was equal to 25.58%

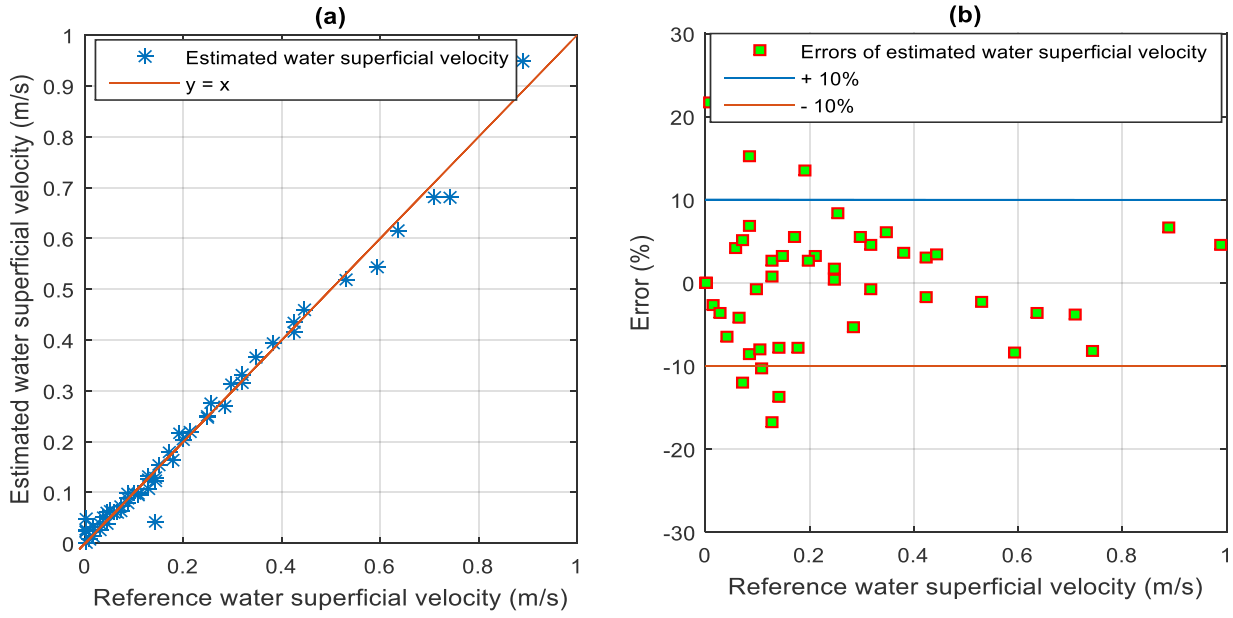
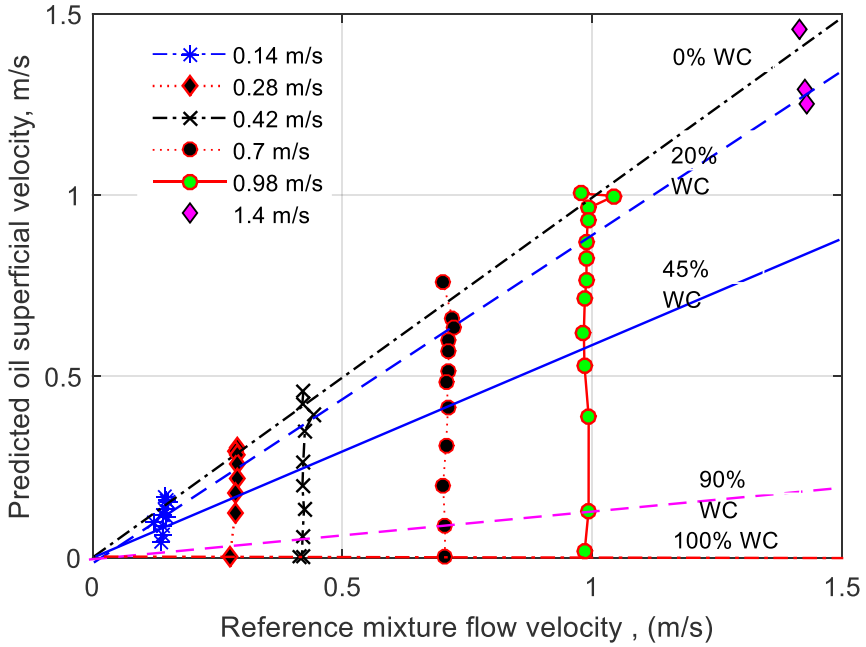


Figure 4-6 (a) the predicted superficial velocity of water by equation (4-4) versus the reference superficial velocity of water (b) the percentage error in superficial velocity of water versus the reference superficial velocity of water

The overall accuracy on the superficial phase velocities estimated have average relative errors of around 4.5% for oil flow velocity, and 5.9% for water flow velocity. However, the error of superficial oil flow velocity estimation rose when the water-cut increased at the initial stages but the relative error decreased as the water cut increased up further. These suggest that that smaller fraction of oil enlarges the relative error at the lower water-cut but relative error fell below 10% at the higher water-cut. The error of superficial water flow velocity was also rose at the lower water-cut but decreased when water-cut increases, the error of superficial water flow velocity predictions was much higher at low water-cut. This phenomenon suggests that the input water-cut range affects the prediction accuracy of both superficial flow velocities. Analyses on effect of water-cut on superficial phase flow velocities estimation is provided in section 4.6.

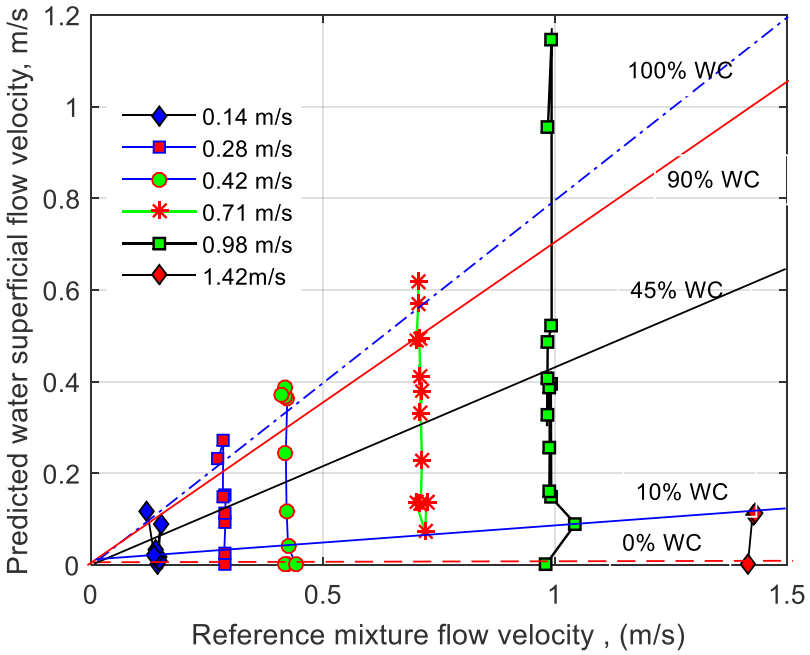
4.5 Superficial velocity of oil and water versus mixture flow velocity

Predicted superficial velocity of oil and of water are reported in Figure 4-5 and Figure 4-6 respectively. Here predicted superficial velocities of oil and of water are reported as a function of the reference mixture flow velocity in Figure 4-7 and Figure 4-8. From the plots, it is evident that oil superficial velocity basically fits the mixture flow velocity data, especially between the water-cut range of 20% and 90%. These translate to a good agreement between Predicted superficial velocity of oil and the oil flow velocity measured with the reference flowmeter in the range tested. A Similar trend was also observed in the comparison of the water superficial velocity and mixture flow velocity measured by the reference flowmeter.



829

830 **Figure 4-7** predicted oil superficial flow velocity versus reference mixture flow velocity



831

832 **Figure 4-8** predicted water superficial flow velocity versus reference mixture flow

833 velocity

834 Figure 4-7 and Figure 4-8 show that prediction of the superficial velocities of oil and water

835 using the drift-flux model has been validated by the results of the reference single phase

836 flowmeters. It is clear from Figure 4-7that the superficial velocity of oil are in accordance with
837 the mixture flow velocity when the oil flow is the continuous, but deviated slightly from the
838 mixture flow velocity as the water-cut increased further. The distribution of the water superficial
839 velocity, however, showed opposite trend. These are slight deviations from the mixture flow
840 velocity are as a result variation in the flow velocity profiles. Oil-water two-phase flow
841 measurement using the CWDU senor in a vertical pipe has not been reported in the literature.

842 ## 4.6 Effect of water-cut on superficial phase flow velocities

843 It is important to note that in this study, both flow rates and water-cuts were varied in
844 order to evaluate meter performance under varying flow conditions. The influence of
845 the water volume fraction data were evaluated based on the errors calculated in the
846 results of both superficial velocities of oil flow and water flow. The errors are the
847 difference between the single phase flow measured at the inlet and results obtained from
848 the proposed method. The phase superficial velocities dependent on both the in situ
849 holdup and the mixture flow velocity. The variation of relative error (ε)of mean oil
850 superficial flow velocity and mean water superficial flow velocity (expressed in per cent
851 of deviation from the inlet measurement) versus water-cut at the inlet are shown in
852 Figure 4-9 (a) and (b).
853

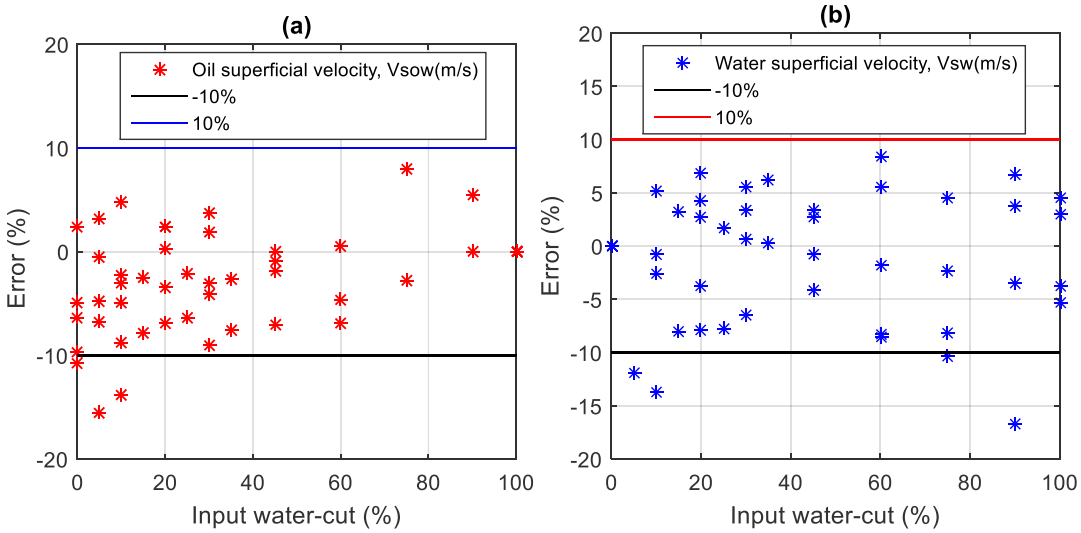


Figure 4-9 Relative error (ε) of mean in phase superficial flow velocities ($V_{so-mean}$ and $V_{sw-mean}$) versus input water-cut

However, experimental results in an inclined pipe by (Lucas and Jin, 2001) who predicted the superficial velocities of oil and water by using a differential pressure measurement and drift-flux model, showed markedly scatter in the data due to variation in the water-cut. But the effect of water-cut variation on the phase flow velocity is not so large within the present experimental condition.

It is interesting to note, the errors encountered in the measurement of water phase flow velocity were at low total flow rate and low water-cut. However, increasing the total flow rate reduces the water phase measurement errors. While the errors encountered in the measurement of the oil phase flow were very high at both very low water-cut (<20%) and very high water-cut (>80%). It was concluded that these trends in the errors were due to increased turbulence in the pipe. Turbulent flow generates random radial movement of the droplets therefore it is a contributory factor in the inaccuracy of the measurement.

5 Conclusions

This paper presents a method for measuring the mixture and individual phase velocities in oil-water two-phase vertical pipe flows using a continuous wave Doppler ultrasonic (CWDU) flow sensor, a gamma densitometer and theoretical correlations based on velocity profiles and the drift-flux model. It was verified and assessed in both the water-continuous flows and oil-continuous flows in a near-industrial scale test rig with the use of industry standard single phase flow meters as references. Errors between the measured oil and water phase flow velocities and those of the respective flow meters are calculated in terms of mean relative error and maximum relative error between the test flowmeters and the reference flowmeters.

The velocity of sound in oil and in water is different. Therefore, we adopted a hybrid method of estimating the sound velocity of the mixture flow which encompasses the contributions of the phase fractions based on the homogenous flow model. The sound speed of the oil-water mixture flow play is vital to the ultrasonic Doppler technique in the flow velocity measurement.

The differences between flow rates obtained from the proposed method and the reference single phase flowmeters depend on the total flow rate as well as the water-cut. The maximum relative differences were found at the low end of the flow rates. The values of the oil-water two-phase flow such as the mixture density, sound speed, and viscosity are estimated based on the homogeneous flow model to simplify the calculation of the theoretical models. These models depend on phase volume fraction estimation. Therefore, the calibration of the gamma densitometer has to be made very accurately or else the estimated flow rates can have significant errors.

In general this oil-water two-phase flow measurement technique developed has effective range when the water volume fraction was between 25% and 75%. This proposed system is entirely non-invasive without utilising any electrical conductance sensor as in in the previous studies(Faraj et al., 2015; Jin et al., 2020; Tan et al., 2016). Therefore, it could be implemented in the pipeline without breaking in the pipeline. Further studies are recommended to focus on experimental investigations using crude oil (instead of mineral) and saline water (instead of tap water) to simulate more practical field conditions of the oil water flows in production operations.

6 References

Abbagoni, B.M., Yeung, H., 2016. Non-invasive classification of gas-liquid two-phase horizontal flow regimes using an ultrasonic Doppler sensor and a neural network. Meas. Sci. Technol. 27. https://doi.org/10.1088/0957-0233/27/8/084002

API, M., 2015. Chapter 8.2- Manual Sampling of Petroleum and Petroleum Products, in: API Manual of Petroleum Measurement Standards Standard Practice for Automatic Sampling of Petroleum and Petroleum Products. API Publishing services, Washington D.C, United State.

Baker, D.W., Yates, G.W., 1973. Technique for studying the sample volume of ultrasonic Doppler devices. Med. Biol. Eng. 766–770.

Bannwart, A.C., 2001. Modeling aspects of oil – water core – annular flows. J. Pet. Sci. Eng. 32, 127–143.

Brauner, N., 2002. Liquid-Liquid Two-Phase Flow Systems, in: Bertola, V. (Ed.),. Udine, Italy, pp. 1–59.

Brauner, N., Ullmann, A., 2002. Modeling of phase inversion phenomenon in two-phase pipe flows. Int. J. Multiph. Flow 28, 1177–1204.

Brody, W.R., Meindl, J.D., James, D., 1974. Theoretical analysis of the CW doppler ultrasonic flowmeter. IEEE Trans. Biomed. Eng. 21, 183–192. https://doi.org/10.1109/TBME.1974.324381

Case, M., Micheli, M., Arroyo, D., Hillard, J., Kocanda, M., 2013. Ultrasonic blood flow sensing using doppler velocimetry. Int. J. smart Sens. Intell. Syst. 6, 1298–1316.

Çengel, Y.A., 2007. Flow in pipes, in: Heat and Mass Transfer: A Practical Approach. McGraw-Hill, Pennsylvania State University, pp. 321–343.

Chaudhuri, A., Sinha, D.N., Zalte, A., Pereyra, E., Webb, C., Gonzalez, M.E., 2014. Mass fraction measurements in controlled oil-water flows using noninvasive ultrasonic sensors. J. Fluids Eng. 136, 1–8. https://doi.org/10.1115/1.4026055

Chemlou, N.S., Chaib, K., Mostefa, K., 2009. Simultaneous measurements of the solid particles velocity and concentration profiles in two phase flow by pulsed ultrasonic Doppler velocimetry. J. Braz. Soc. Mech. Sci. Eng. XXXI, 333–343.

Chen, J., Xu, L., Cao, Z., Zhang, W., Liu, X., 2015. Water cut measurement of oil – water flow in vertical well by combining total flow rate and the response of a conductance probe. Meas. Sci. Technol. 10pp. https://doi.org/10.1088/0957-0233/26/9/095306

Da, N., Sirivat, A., Siemanond, K., Wilkes, J.O., 2007. Vertical two-phase flow regimes and pressure gradients : Effect of viscosity. Exp. Therm. Fluid Sci. 31, 567–577. https://doi.org/10.1016/j.expthermflusci.2006.03.030

Descamps, M., Oliemans, R.V.A., Ooms, G., Mudde, R.F., Kusters, R., 2006. Influence of gas injection on phase inversion in an oil – water flow through a vertical tube. Int. J. Multiph. Flow 32, 311–322.

941 https://doi.org/10.1016/j.ijmultiphaseflow.2005.10.006
942 Dong, X., Tan, C., Yuan, Y., Dong, F., 2016. Measuring oil – water two-phase flow
943 velocity with continuous-wave ultrasound Doppler sensor and drift-flux model.
944 IEEE Trans. Instrum. Meas. 65, 1–10.
945 Dong, X., Tan, C., Yuan, Y., Dong, F., 2015. Oil – water two-phase fl ow velocity
946 measurement with continuous wave ultrasound Doppler. Chem. Eng. Sci. 135,
947 155–165. https://doi.org/10.1016/j.ces.2015.05.011
948 Du, M., Jin, N., Gao, Z., Wang, Z., Zhai, L., 2012. Flow pattern and water holdup
949 measurements of vertical upward oil – water two-phase flow in small diameter
950 pipes. Int. J. Multiph. Flow 41, 91–105.
951 https://doi.org/10.1016/j.ijmultiphaseflow.2012.01.007
952 Eskin, D., Taylor, S., Mark, S., Abdallah, W., 2017. Modeling droplet dispersion in a
953 vertical turbulent tubing flow. Chem. Eng. Sci. 173, 12–20.
954 https://doi.org/10.1016/j.ces.2017.07.023
955 Falcone, G., Hewitt, G.F., Alimonti, C., 2009. Multiphase flow metering: principles and
956 applications, First edit. ed. Elsevier Science, Oxford, United Kingdom.
957 Faraj, Y., Wang, M., Jia, J., Wang, Q., Xie, C., Oddie, G., Primrose, K., Qiu, C., 2015.
958 Measurement of vertical oil-in-water two-phase flow using dual-modality ERT –
959 EMF system. Flow Meas. Instrum. 46, 255–261.
960 https://doi.org/10.1016/j.flowmeasinst.2015.08.010
961 Figueiredo, M.M.F., Goncalves, J.L., Nakashima, A.M. V, Fileti, A.M.F., Carvalho,
962 R.D.M., 2016. The use of an ultrasonic technique and neural networks for
963 identification of the flow pattern and measurement of the gas volume fraction in
964 multiphase flows. Exp. Therm. Fluid Sci. 70, 29–50.

https://doi.org/10.1016/j.expthermflusci.2015.08.010

Flores, J., Chen, X., Sarica, C., Brill, J., 1999. Characterization of oil–water flow patterns in vertical and deviated wells, in: SPE Annual Technical Conference and Exhibition. SPE, San Antonio, Texas, pp. 5–8. https://doi.org/10.2118/56108-PA

Flores, J.G., Sarica, C., Chen, T.X., Brill, J.P., 1998. Investigation of holdup and pressure drop behavior for oil-water flow in vertical and deviated wells. J. Energy Resour. Technol. 120, 8–14.

Garcia-Lopez, A., Sinha, D.N., 2008. Enhanced acoustic separation of oil-water emulsion in resonant cavities. Open Acoust. J. 1, 66–71.

Grassi, B., Strazza, D., Poesio, P., 2008. Experimental validation of theoretical models in two-phase high-viscosity ratio liquid – liquid flows in horizontal and slightly inclined pipes. Int. J. Multiph. Flow 34, 950–965. https://doi.org/10.1016/j.ijmultiphaseflow.2008.03.006

Harmathy, T.Z., 1960. Velocity of Large Drops and Bubbles in Media of Infinite or Restricted Extent. Am. Inst. Chem. Eng. J.

Hasan, A.R., Kabir, C.S., 1998. A simplified model for oil-water flow in vertical and deviated wellbores, in: SPE Annual Technical Conference and Exhibition. New Orleans, Louisiana,.

Hu, B., Matar, O.K., Hewitt, G.F., Angeli, P., 2007. Mean and turbulent fluctuating velocities in oil – water vertical dispersed flows. Chem. Eng. Sci. 62, 1199–1214. https://doi.org/10.1016/j.ces.2006.10.008

Huang, S., Xie, C., Lenn, C., Yang, W., Wu, Z., 2013. Issues of a combination of ultrasonic Doppler velocity measurement with a venturi for multiphase flow metering, in: The SPE Middle East Oil and Gas Show and Conference Held.

989 Society of Petroleum Engineers, Manama, pp. 1–9.
990 Ibarra, R., Zadrazil, I., Matar, O.K., Markides, C.N., 2017. Dynamics of liquid-liquid
991 flows in horizontal pipes using simultaneous two-line planar laser-induced
992 fluorescence and particle velocimetry. Int. J. Multiph. Flow.
993 https://doi.org/10.1016/j.ijmultiphaseflow.2017.12.018
994 Ismail, I., Gamio, J.C., Bukhari, S.F.A., Yang, W.Q., 2005. Tomography for multi-
995 phase flow measurement in the oil industry. Flow Meas. Instrum. 16, 145–155.
996 https://doi.org/10.1016/j.flowmeasinst.2005.02.017
997 Jana, A.K., Das, G., Das, P.K., 2006. Flow regime identification of two-phase liquid –
998 liquid upflow through vertical pipe. Chem. Eng. Sci. 61, 1500–1515.
999 https://doi.org/10.1016/j.ces.2005.09.001
1000 Jin, N., Yu, C., Han, Y., Yang, Q., Ren, Y., Zhai, L., 2020. The performance
1001 characteristics of electromagnetic flowmeter in vertical low-velocity oil-water two-
1002 phase flow. IEEE sensors 21, 464–475.
1003 https://doi.org/10.1109/JSEN.2020.3013327
1004 Kikura, H., Yamanaka, G., Aritomi, M., 2004. Effect of measurement volume size on
1005 turbulent flow measurement using ultrasonic Doppler method. Exp. Fluids 36,
1006 187–196. https://doi.org/10.1007/s00348-003-0694-x
1007 Kouame, D., Girault, J., Remenieras, J., Chemla, J.-P., Marc, L., 2003. High resolution
1008 processing techniques for ultrasound Doppler velocimetry in the presence of
1009 colored noise . Part II : multiple phase pipe-flow velocity measurement. IEEE
1010 Trans. Ultrason. Ferroelectr. Freq. Control 50.
1011 Kudela, H., 2010. Turbulent flow, in: Pdf Document. availabe at
1012 http://www.itcmp.pwr.wroc.pl/~znmp/dydatyka/fundam_FM/Lecture_no3_Turbule

1013 nt_Flow_Modelling.pdf. Accessed on 15/04/2019
1014 Kumara, W.A.S., Halvorsen, B.M., Melaaen, M.C., 2010a. Single-beam gamma
1015 densitometry measurements of oil–water flow in horizontal and slightly inclined
1016 pipes. Int. J. Multiph. Flow 36, 467–480.
1017 Kumara, W.A.S., Halvorsen, B.M., Melaaen, M.C., 2010b. Single-beam gamma
1018 densitometry measurements of oil – water flow in horizontal and slightly inclined
1019 pipes. Int. J. Multiph. Flow 36, 467–480.
1020 https://doi.org/10.1016/j.ijmultiphaseflow.2010.02.003
1021 Kumara, W.A.S., Halvorsen, B.M., Melaaen, M.C., 2010c. Particle image velocimetry
1022 for characterizing the flow structure of oil – water flow in horizontal and slightly
1023 inclined pipes. Chem. Eng. Sci. 65, 4332–4349.
1024 https://doi.org/10.1016/j.ces.2010.03.045
1025 Kumara, W.A.S., Halvorsen, B.M., Melaaen, M.C., 2009. Pressure drop flow pattern
1026 and local water volume fraction measurements of oil-water flow in pipes. Meas.
1027 Sci. Technol. 1–25.
1028 Liu, W., Tan, C., Dong, F., 2021. Doppler spectrum analysis and flow pattern
1029 identification of oil-water two-phase flow using dual-modality sensor. Flow Meas.
1030 Instrum. 77, 101861. https://doi.org/10.1016/j.flowmeasinst.2020.101861
1031 Liu, Y., Deng, Y., Zhang, M., Yu, P., Li, Y., 2017. Experimental measurement of oil –
1032 water two-phase flow by data fusion of electrical tomography sensors and venturi
1033 tube. Meas. Sci. Technol. 28, 15.
1034 Lovick, J., Angeli, P., 2004. Experimental studies on the dual continuous flow pattern in
1035 oil – water flows. Int. J. Multiph. Flow 30, 139–157.
1036 https://doi.org/10.1016/j.ijmultiphaseflow.2003.11.011

1037 Lucas, G.P., Jin, N.D., 2001. Investigation of a drift velocity model for predicting
1038 superficial velocities of oil and water in inclined oil-in-water pipe flows. Meas.
1039 Sci. Technol. 12, 1546–1554.
1040 Mazza, R.A., Suguimoto, F.K., 2019. Journal of Petroleum Science and Engineering
1041 Experimental investigations of kerosene-water two-phase flow in vertical pipe. J.
1042 Pet. Sci. Eng. 106580. https://doi.org/10.1016/j.petrol.2019.106580
1043 Meribout, M., Al-Rawahi, N.Z., Al-Naamany, A.M., Al-Bimani, A., Al-Busaidi, K.,
1044 Meribout, A., 2010. A Multisensor intelligent device for real-time multiphase flow
1045 metering in oil fields. Instrum. Meas. IEEE Trans. 59, 1507–1519.
1046 Morriss, S.L., Hill, A.D., 1991. Measurement of velocity profiles in upwards oil/water
1047 flow using ultrasonic Doppler velocimetry, in: SPE Annual Technical Conference
1048 and Exhibition. Dallas, TX.
1049 Murai, Y., Tasaka, Y., Nambu, Y., Takeda, Y., A, S.R.G., 2010. Ultrasonic detection of
1050 moving interfaces in gas – liquid two-phase flow. Flow Meas. Instrum. 21, 356–
1051 366. https://doi.org/10.1016/j.flowmeasinst.2010.03.007
1052 Oddie, G.M., 1992. On the detection of a low-dimensional attractor in disperse two-
1053 component (oil-water) flow in a vertical pipe 2, 225–231.
1054 Onda, C., 2003. Acoustic Properties of Liquids.
1055 Paolinelli, L.D., 2020. A comprehensive model for stability of dispersed oil-water flow
1056 in horizontal and inclined pipes. Chem. Eng. Sci. 211, 115325.
1057 https://doi.org/10.1016/j.ces.2019.115325
1058 Picchi, D., Strazza, D., Demori, M., Ferrari, V., Poesio, P., 2015. An experimental
1059 investigation and two-fluid model validation for dilute viscous oil in water
1060 dispersed pipe flow. Exp. Therm. Fluid Sci. 60, 28–34.

https://doi.org/10.1016/j.expthermflusci.2014.07.016

Rodriguez, O.M.H., Oliemans, R.V.A., 2006. Experimental study on oil – water flow in horizontal and slightly inclined pipes. Int. J. Multiph. Flow 32, 323–343. https://doi.org/10.1016/j.ijmultiphaseflow.2005.11.001

Rothfuss, M.A., Unadkat, J. V., Gimbel, M.L., Mickle, M.H., Sejdi, E.C., 2016. Totally implantable wireless ultrasonic Doppler blood flowmeters : toward accurate miniaturized chronic monitors. Ultrasound Med. Biol. 1–18. https://doi.org/10.1016/j.ultrasmedbio.2016.11.005

Sanderson, M.L., Yeung, H., 2002. Guidelines for the use of ultrasonic non-invasive metering techniques. Flow Meas. Instrum. 13 13, 125–142.

Shamsul, A., Ismail, Izwan, Ismail, Issham, Zoveidavianpoor, M., 2015. Review of oil – water through pipes. Flow Meas. Instrum. 45, 357–374. https://doi.org/10.1016/j.flowmeasinst.2015.07.015

Shi, X., Dong, X., Tan, C., Dong, F., 2017. Velocity measurement of oil-water two-phase flow based on ultrasonic Doppler. IEEE Trans. Instrum. Meas.

Stahl, P., von Rohr, P.R., 2004. On the accuracy of void fraction measurements by single-beam gamma-densitometry for gas–liquid two-phase flows in pipes. Exp. Therm. Fluid Sci. 28, 533–544.

Tan, C., Dai, W., Yeung, H., Dong, F., 2015. A Kalman estimation based oil – water two-phase flow measurement with CRCC. Int. J. Multiph. Flow 72, 306–317. https://doi.org/10.1016/j.ijmultiphaseflow.2014.06.014

Tan, C., Murai, Y., Liu, W., Tasaka, Y., Dong, F., Takeda, Y., 2021. Ultrasonic Doppler Technique for Application to Multiphase Flows : A Review. Int. J. Multiph. Flow. https://doi.org/10.1016/j.ijmultiphaseflow.2021.103811

Tan, C., Yuan, Y., Dong, X., Dong, F., 2016. Oil-water two-phase flow measurement with combined ultrasonic transducer and electrical sensors. Meas. Sci. Technol. 27. https://doi.org/10.1088/0957-0233/27/12/125307

Tesi, A.I.M., 2011. Multiphase flow measurement using gamma-based techniques, PhD Thesis,. Cranfield University.

Thorn, R., Johansen, G.A., Hjertaker, B.T., 2013. Three-phase flow measurement in the petroleum industry. Meas. Sci. Technol. 24, 17. https://doi.org/10.1088/0957-0233/24/1/012003

Wallis, G.B., 1969. One Dimensional Two-Phase Flow. McGraw Hill Book Co. Inc., New York City.

Yin, P., Cao, X., Zhang, P., Yang, W., Bian, J., Guo, D., 2019. Investigation of slug flow characteristics in hilly terrain pipeline using ultrasonic Doppler method. Chem. Eng. Sci. 115300. https://doi.org/10.1016/j.ces.2019.115300

Zhai, L., Jin, N., Gao, Z., Wang, Z., Li, D., 2013. The ultrasonic measurement of high water volume fraction in dispersed oil-in-water flows. Chem. Eng. Sci. 94, 271–283. https://doi.org/10.1016/j.ces.2013.02.049

7 Appendix

7.1 Solution to equation (2-28)

$$\bar{v}_{dop} = 2.5\mathrm{u}_\tau \ln\frac{\mathrm{u}_\tau \rho_m R}{\mu_m} + 1.75\mathrm{u}_\tau \tag{A-1}$$

$$\bar{v}_{dop} = B\mathrm{u}_\tau \ln K\mathrm{u}_\tau + A\mathrm{u}_\tau \tag{A-2}$$

$$B = 2.5,\ A = 1.75,\ K = \frac{\rho_m R}{\mu_m}$$

*E*quation **(A-1)** *can be solved in similar expansion method as in* Tan et al. (2016). *The expansion* $\mathrm{Ln}\, x = (x-1) + \sum_{n=0}^{\infty} \frac{(-1)^n (x-1)^n}{n+1} \approx x - E$ *was used to transform the equation* (A-2) *as :*

$$Bu_t^2 + (A + BlnK - B * E)\mathrm{u}_\tau - \bar{v}_{dop} = 0 \qquad \text{(A-3)}$$

$$a = B$$

$$b = A + BlnK - B * E$$

$$c = -\bar{v}_{dop}$$

E is a compensation coeffiient, which is dependednt on the nature of the flow. In this study, most of the experiments are in dispearsed flow and the value of $E = 3.3$ for a dispersed flow (Tan et al., 2016).

Solving the quadratic equation (A-3), the following expression for u_τ, the shear velocity can be obtained:

$$u_\tau = \frac{-b + \sqrt{b^2 - 4ac}}{2a} \qquad \text{(A-4)}$$

Finally, the mixture velocity $\mathrm{V_m}$ can be calculated from the Eqn. (2-29)

8 Acknowledgements

We are grateful for the sponsorship from the Petroleum technology development fund (PTDF, Nigeria) under the overseas scholarship scheme for PhD programme at Cranfield University. Dr Baba Musa Abbagoni is particularly thankful to the PTDF for sponsoring his postgraduate studies.

Nomenclature

$\overline{f_d}$	average frequency shift reflected by the multiple droplets
$\mathrm{E_r}$	relative error of the estimation

ε_{ave}	average absolute of the error of the estimation
A_p	pipe cross-sectional area, m^2
C_o	flow distribution parameter,
I_0	Initial gamma intensity
U_{ow}	drift flux between the phases
V_∞	Terminal rise velocity
c_{ow}	sound speed in the oil/water mixture
f_m	two-phase friction factor
f_{max}	maximum Doppler frequency
f_t	transmitted frequency
k_m	mixture compressibility
u^+	dimensionless velocity
u_τ	shear velocity m/s
$\overline{v}$	Average velocity of droplets in the measuring volume
y^+	dimensionless wall distance
ρ_m	mixture density
D	flow pipe internal diameter, m
DP	differential pressure
E	compensation coefficient
I	received gamma intensity
$P(f)$	Doppler power spectrum
Q	volume flow rate (oil + water)
Re	Reynolds number, dimensionless

V	measured mean superficial flow velocity
V	measured mean superficial flow velocity
b	friction factor's coefficient
c	speed of the sound,
g	acceleration due to gravity
k	compressibility
m	Exponent of the drift velocity,
n	friction factor's exponent
$u(ow)$	flow velocity profile
z	distance gamma ray travelled through the absorbing medium

Greek letters

σ_{ow}	interracial tension,
φ_a	linear absorption coefficient in the air
φ_o	linear absorption coefficient for oil
φ_p	linear absorption coefficient in the pipe wall material
φ_w	linear absorption coefficient for water
z	distance travelled through the absorbing medium
Φ	is the angle of inclination of the flow pipe from the horizontal.
α	time-averaged local volume fraction
θ	angle between the ultrasonic beam and the pipe axis
μ	dynamic viscosity
ρ	flow density,
τ	wall shear stress,

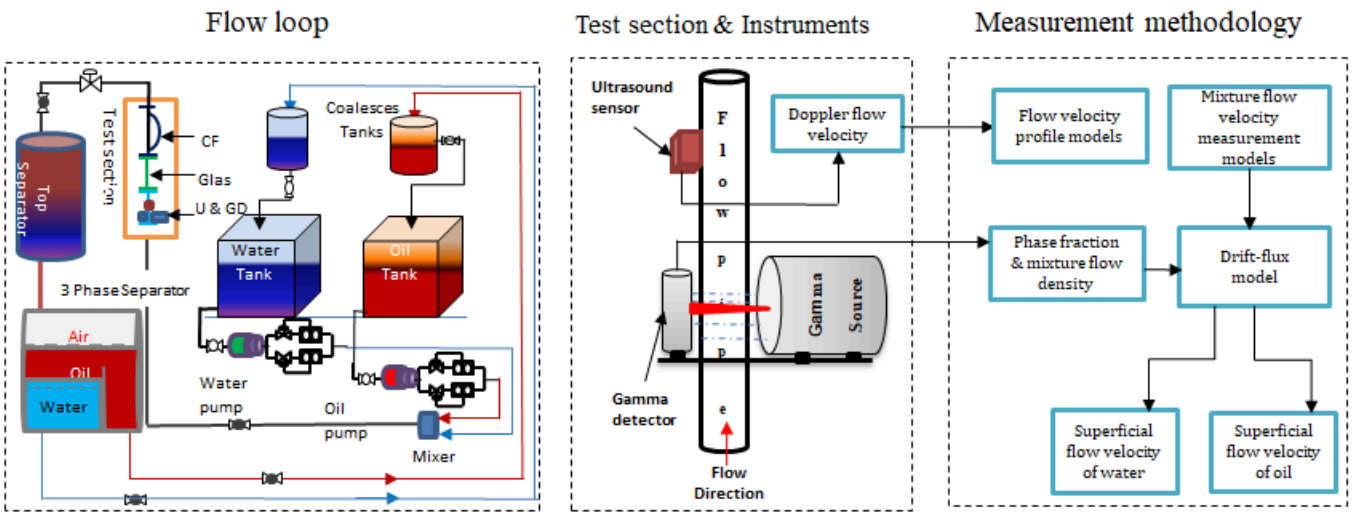
φ	gamma absorption coefficient;

Subscripts

m	oil-water mixture
o	oil flow phase
so	superficial for oil phase
sw	superficial for water phase
w	water flow phase
z	distance travelled through the absorbing medium

Subscripts

m	oil-water mixture
o	oil flow phase
so	superficial for oil phase
sw	superficial for water phase
w	water flow phase



Graphical abstract

Highlights

- A method of measurement of of flow velocity in oil-water two-phase vertical flow using a non-invasive ultrasound Doppler sensor is developed
- We present flow velocity measurement correlations for both oil-continuous flow and water-continuous flow
- We formulated the drift-flux model for estimation of superficial velocity of oil and of water from the measured two-phase flow velocity.
- The estimated results using this proposed method are in good agreement with the reference flowmeters.

DSPACE

https://dspace.org/

Non-invasive measurement of oil-water two-phase flow in vertical pipe using ultrasonic Doppler sensor and gamma ray densitometer

Abbagoni, Baba Musa; Yeung, Hoi; Lao, Liyun

2021-10-28
Elsevier
https://doi.org/10.1016/j.ces.2021.117218
Abbagoni BM, Yeung H, Lao L. (2022) Non-invasive measurement of oil-water two-phase flow in vertical pipe using ultrasonic Doppler sensor and gamma ray densitometer. Chemical Engineering Science, Volume 248, Part B, February 2022, Article number 117218

Downloaded from a DSpace repository. https://dspace.org/